

Article

Discovery of Novel 11-Triazole Substituted Benzofuro[3,2-b]quinolone Derivatives as c-myc G-Quadruplex Specific Stabilizers via Click Chemistry

De-Ying Zeng, Guo-Tao Kuang, Shi-Ke Wang, Wang Peng, Shu-Ling Lin, Qi Zhang, Xiao-Xuan Su, Ming-Hao Hu, Honggen Wang, Jia-Heng Tan, Zhi-Shu Huang, Lian-Quan Gu, and Tian-Miao Ou

J. Med. Chem., **Just Accepted Manuscript** • Publication Date (Web): 17 May 2017

Downloaded from <http://pubs.acs.org> on May 18, 2017

Just Accepted

“Just Accepted” manuscripts have been peer-reviewed and accepted for publication. They are posted online prior to technical editing, formatting for publication and author proofing. The American Chemical Society provides “Just Accepted” as a free service to the research community to expedite the dissemination of scientific material as soon as possible after acceptance. “Just Accepted” manuscripts appear in full in PDF format accompanied by an HTML abstract. “Just Accepted” manuscripts have been fully peer reviewed, but should not be considered the official version of record. They are accessible to all readers and citable by the Digital Object Identifier (DOI®). “Just Accepted” is an optional service offered to authors. Therefore, the “Just Accepted” Web site may not include all articles that will be published in the journal. After a manuscript is technically edited and formatted, it will be removed from the “Just Accepted” Web site and published as an ASAP article. Note that technical editing may introduce minor changes to the manuscript text and/or graphics which could affect content, and all legal disclaimers and ethical guidelines that apply to the journal pertain. ACS cannot be held responsible for errors or consequences arising from the use of information contained in these “Just Accepted” manuscripts.

1
2
3 **Discovery of Novel 11-Triazole Substituted Benzofuro[3,2-b]quinolone**
4
5 **Derivatives as *c-myc* G-Quadruplex Specific Stabilizers via Click**
6
7 **Chemistry**
8
9

10
11
12
13
14 De-Ying Zeng†, Guo-Tao Kuang†, Shi-Ke Wang, Wang Peng, Shu-Ling Lin, Qi
15
16 Zhang, Xiao-Xuan Su, Ming-Hao Hu, Honggen Wang, Jia-Heng Tan, Zhi-Shu Huang,
17
18 Lian-Quan Gu, Tian-Miao Ou*
19

20
21
22
23
24
25 *School of Pharmaceutical Sciences, Sun Yat-sen University, Guangzhou 510006,*
26
27 *People's Republic of China.*
28
29
30
31
32
33
34
35
36
37
38
39
40
41
42
43
44
45
46
47
48
49
50
51
52
53
54
55
56
57
58
59
60

ABSTRACT

The specificity of nucleic acids' binders is crucial for developing this kind of drugs, especially for novel G-quadruplexes' binders. Quindoline derivatives have been developed as G-quadruplex stabilizers with good interactive activities. In order to improve the selectivity and binding affinity of quindoline derivatives as *c-myc* G-quadruplex binding ligands, novel triazole containing benzofuroquinoline derivatives (**T-BFQs**) were designed and synthesized by using the 1,3-dipolar cycloaddition of a series of alkyne and azide building blocks. The selectivity towards *c-myc* G-quadruplex DNA of these novel **T-BFQs** was significantly improved, together with an obvious increase on binding affinity. Further cellular and *in vivo* experiments indicated that the **T-BFQs** showed inhibitory activity on tumor cells' proliferation, and presumably through the down-regulation of transcription of *c-myc* gene. Our findings broadened the modification strategies of specific G-quadruplex stabilizers.

KEYWORDS

c-myc gene; G-quadruplex; benzofuro[3,2-*b*]quinolone derivatives; click chemistry; antitumor.

■ INTRODUCTION

Guanine-rich DNA sequences are able to fold into four-stranded secondary structures known as G-quadruplexes which arise from guanine DNA bases self-association by Hoogsteen hydrogen bonds.¹⁻² The G-quadruplex structures have drawn extensive attention, as the putative quadruplex sequences (PQS) are widespread throughout the human genome, notably in telomeres and the promoter region of oncogenes such as *c-kit* and *c-myc*.³⁻⁴ With great biological and therapeutic significance, G-quadruplexes are now perceived as promising drug targets.⁵

c-myc is an important proto-oncogene that plays a crucial role in cell growth, cellular proliferation, and apoptosis. Aberrant overexpression of the *c-myc* gene is closely related to the occurrence and the development of various cancers.⁶ The nuclease hypersensitivity element III₁ (NHE III₁), located at 142-115 bp upstream from the P1 promoter of *c-myc* gene, is a guanine-rich sequence that can form intramolecular G-QUADRUPLEX structures.⁷⁻⁸ These intramolecular G-quadruplex structures can act as a repressor of the *c-myc* transcription level.⁹⁻¹⁰ Specific G-quadruplex binders that can promote formation or enhance the stability of the G-quadruplex could, in turn, inhibit the transcription activity and down-regulate the expression of *c-myc* gene.¹¹⁻¹² Thus, the design of drugs specifically interacting at the *c-myc* G-quadruplex could pave the way for the discovery of novel anti-cancer agents. Several small molecules have been reported with the ability to interact with *c-myc* G-quadruplex, including porphyrin analogs,¹¹ berberine derivatives,¹³ quindoline derivatives,¹² and hydrazone derivatives.¹⁴

Quindoline derivatives have been developed as effective G-quadruplexes' ligands and optimized in several ways (Figure 1A).^{12, 15-21} The planar and aromatic

1
2
3 scaffold of the quindoline provides good recognition for G-quartet through π - π
4 stacking interactions. In addition, the introduction of an amino side chain on the
5 11-position,^{18, 21} the introduction of a positive charge by methylation at the 5-N
6 position of 7-fluorinated quindoline derivatives,¹⁷ and the introduction of a peptidyl
7 group at the 11-position of the aromatic benzofuroquinoline scaffold,¹⁶ lead to
8 significant improvement of their binding affinity to G-quadruplex. Although these
9 compounds show interactions with the G-quadruplex in the *c-myc* gene with certain
10 selectivity,^{12, 18, 22} the specificities of this kind of compounds still need to be
11 improved.
12
13

14
15
16
17
18
19
20
21
22
23 According to the representative model of the quindoline-G-quadruplex complex
24 structure,²² the short protonated amino alkyl side chain attached to the quindoline
25 skeleton is barely able to reach the nearest groove. Therefore, the modification in the
26 present study is aim to solve this problem.
27
28
29
30

31
32 The heteroaromatic 1,4-substituted 1,2,3-triazole ring system has attracted
33 extensive interest in drug design, owing to its wide application as a synthetic building
34 block endowed with pharmacological potential.²³⁻²⁴ A variety of triazole-linked
35 groups leads to a better selectivity.²⁵⁻²⁸ Therefore, we designed a series of 11-triazole
36 benzofuroquinoline derivatives (**T-BFQ**, Figure 1B) to enhance the affinity and
37 selectivity of these derivatives for targeting *c-myc* G-quadruplex structure. In addition,
38 we took advantage of the CuAAC click chemistry reaction for extending the diversity
39 of the substituents,²⁹ including groups with varying properties and linker lengths
40 which comprise open-chain amino groups (series **a**), azo-heterocyclic rings (series **a**),
41 hydroxyl group (series **b**), phenyl group (series **b**), etc.
42
43
44
45
46
47
48
49
50
51
52

53
54 Panels of experiments were applied to evaluate the effects of these **T-BFQ**
55 derivatives. We found that the introduction of the triazole moiety could not only
56
57
58
59
60

enhance their binding affinities, but also significantly improved the selectivity toward *c-myc* G-quadruplex. The combined results of these studies led to a structure-activity relationship that amino substituents and a longer side chain length are important for improvement of their specific interactions with the *c-myc* G-quadruplex. Further biological experiments showed that the selected derivatives could repress the proliferation of human lymphoma cells, interfere the cell cycle, and presumably through the down-regulation of transcription of *c-myc* gene.

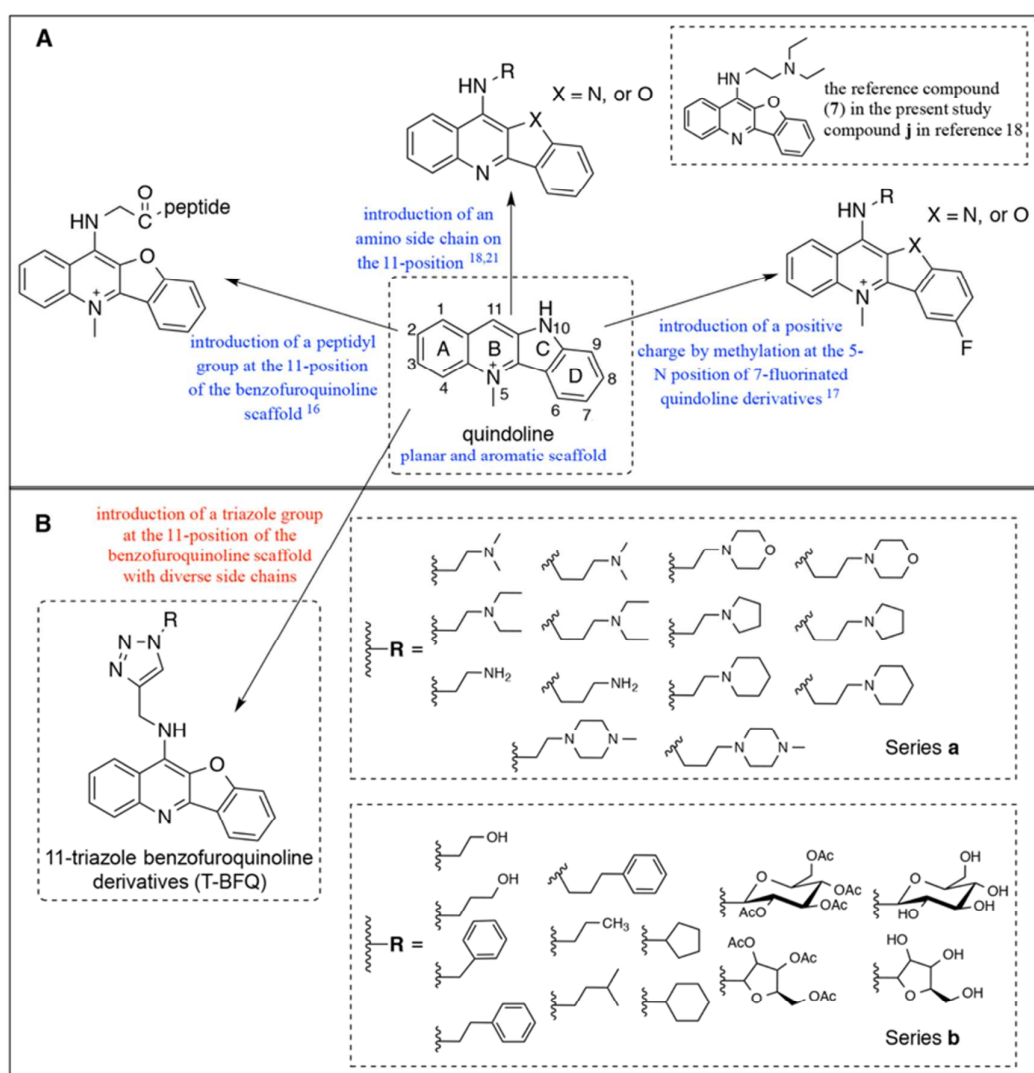
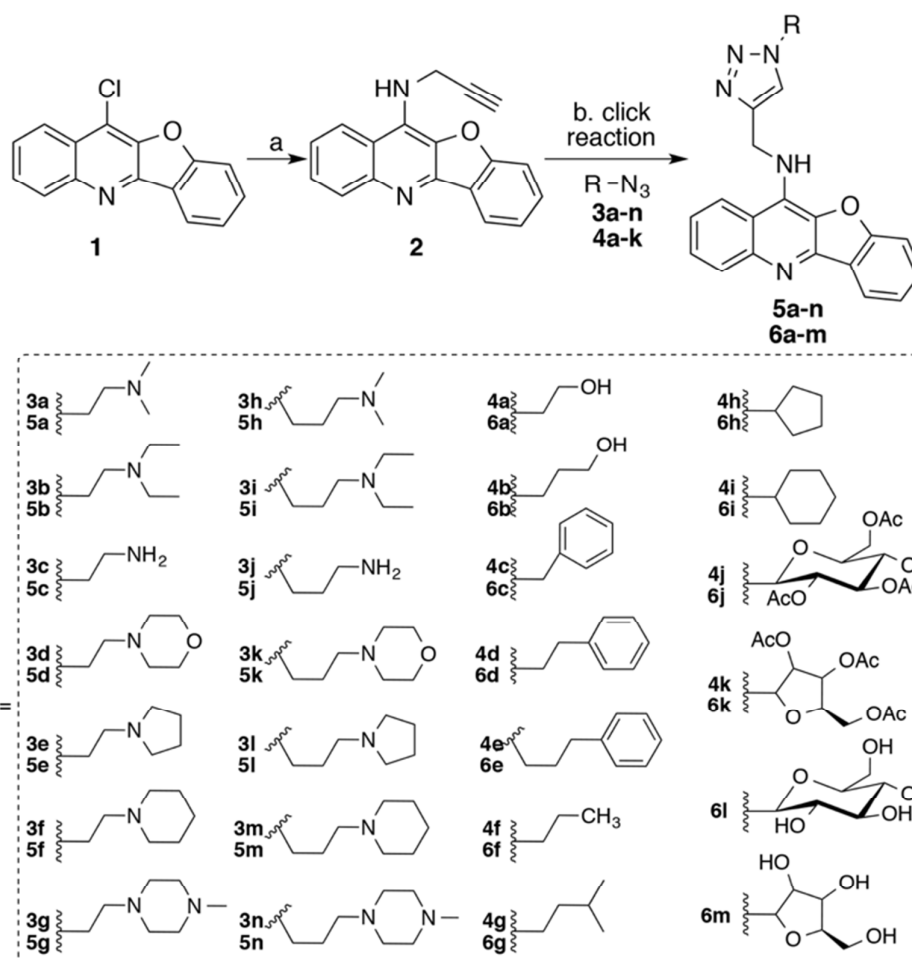


Figure 1. Modification strategies of the quindoline scaffold in previous studies (A) and the present study (B).

■ RESULTS AND DISCUSSION

Chemistry. The synthetic route for the compounds was shown in Scheme 1. The key intermediate of 11-chloroquinoline **1** was prepared following the procedure previously reported.²¹ The azido side chains **3a-3n** and **4a-4k** were synthesized from the commercially available corresponding halide side chains via an azidation reaction with NaN_3 or TMSN_3 (Scheme S1). All azides were directly used for copper(I) catalyzed cycloadditions without any further purification. The 1,3-dipolar cycloaddition was performed with an excess of azido reactants, and CuSO_4 was used as copper source and sodium ascorbate as reducing agent. Most of the click reactions were completed within 12 h at 35 °C to give all the products (**5a-5n** and **6a-6m**).



35
36
37
38
39
40
41
42
43
44
45
46
47
48
49
50
51
52
53
54
55
56
57
58
59
60

Scheme 1. Synthesis of 11-triazole benzofuro[3,2-b]-quinoline derivatives **5a-n**, and **6a-m**. Reagents and conditions: (a) p-TsOH, 2-Propargylamine, 120 °C, 6 hours; (b) Azides **3a-n** and **4a-k**, CuSO₄·5H₂O, sodium ascorbate, THF/H₂O, 35 °C, 6-12 hours.

Thermodynamic Stabilization Abilities of the T-BFQ Derivative on the *c-myc* G-Quadruplex. One of the important properties of a good G-quadruplex ligand should be the stabilizing ability on quadruplex-forming sequence. Fluorescence resonance energy transfer (FRET) assay was used to investigate the stabilizing ability of T-BFQ derivatives on the G-quadruplex DNA in the *c-myc* gene promoter. The promoter G-quadruplex sequence of *c-myc* containing a FAM label at 5' and a TAMRA (carboxytetramethylrhodamine) label at 3' (FPu22T, Table S1) was used. An

1
2
3 oligonucleotide that formed hairpin duplex DNA structure (F10T, Table S1) with
4 similar dual-fluorescence labels was used as a non-quadruplex control. A previously
5 reported quindoline derivative **j** (numbered as **7** in this paper) with the same
6 benzofuroquinoline scaffold (Figure 1A) was used as a reference compound.¹⁸
7
8
9

10
11 The results of T_m (melting temperature) values from the FRET melting
12 experiments were shown in Table 1, and all the original melting curves were shown in
13 Figure S1 and S2. The reference compound **7** could increase the T_m value of FPU22T
14 by 16.0 °C, and increase the T_m value of F10T by 2.6 °C. Comparing with **7**, most
15 **T-BFQ** derivatives in series **a** showed higher ΔT_m on FPU22T while lower ΔT_m on
16 F10T, which implied an improved selectivity of these new compounds. For example,
17 **5a** could increase the T_m value of FPU22T by 22.0 °C, and increase the T_m value of
18 F10T by 1.2 °C, indicating that the incorporation of the triazole moiety enhanced the
19 interaction of the ligand with the G-quadruplex DNA. On the other hand, compounds
20 in series **b** showed diverse activities. Generally, most compounds in series **b** had
21 lower stabilization abilities on both the G-quadruplex DNA and the hairpin DNA than
22 compound **7**.
23
24
25
26
27
28
29
30
31
32
33
34
35
36
37

38 The structure-activity relationships (SAR) could be concluded from the
39 stabilizing activity of the tested compounds toward *c-myc* G-quadruplex. In particular,
40 the introduction of *in situ* protonated terminal substituents (amino groups and
41 azo-heterocyclic rings) in series **a** remarkably increased their G-quadruplex
42 stabilizing efficiency, such as compound **5a**, **5c**, **5i**, and **5j**. In addition, the
43 introduction of monohydroxyl group (**6a** and **6b**) could also result in increased ΔT_m
44 values, while the introduction of polyhydroxyl groups (**6j-6m**), and phenyl groups (**6d**
45 and **6e**), lead to rather weak stabilizing ability which may attribute to their oversize
46 bulk. These results revealed that the terminal substituents of the side chain, especially
47
48
49
50
51
52
53
54
55
56
57
58
59
60

1
2
3 basic amino groups, could significantly enhance their ability of stabilizing
4 G-quadruplex, which was consistent with the previous findings.¹⁸ This was reasonable
5 because electrostatic interaction between the ligand side chain and the G-quadruplex
6 structure was an important factor for the recognition process according to previous
7 researches.^{17, 21} Furthermore, with the same terminal basic substituent, compounds (**5i**,
8 **5k**, **5m**, and **5n**) containing longer side chains showed relatively stronger stabilizing
9 ability to the *c-myc* G-quadruplex than compounds (**5b**, **5d**, **5f**, and **5g**) with shorter
10 side chains. This result reinforced our idea that the ligand-quadruplex interactions
11 would be enhanced by extending side chain to allow deeper penetration of the
12 terminal substituents into the G-quadruplex grooves so that more groove space would
13 be exploited.

14
15
16
17
18
19
20
21
22
23
24
25
26
27
28 To further characterize the selectivity of these **T-BFQ** derivatives, we picked
29 compounds **5a**, **5h**, **5l**, **5n**, and **7** to performed the competitive FRET experiments. In
30 this assay, a non-fluorescent duplex DNA competitor ds26 (Table S1) was used as the
31 competitor in the system containing FPu22T. As shown in Figure 2A, in the presence
32 of excess hairpin competitor (5-25 folds excess), the ΔT_m values of the FPu22T was
33 slightly affected in all the **T-BFQ** derivatives, while dropped dramatically in
34 compound **7**. These results further indicated that the **T-BFQ** derivatives could
35 specifically stabilize G-quadruplex with no significant effect on duplex DNA.

36
37
38
39
40
41
42
43
44
45
46
47
48 **Table 1.** Changes of oligomer's melting temperatures (ΔT_m) obtained
49 from the FRET-melting assay.

50
51
52
53

Cpd.	ΔT_m^a (°C)		Cpd.	ΔT_m (°C)	
	FPu22T	F10T		FPu22T	F10T

54
55
56
57
58
59
60

5a	22.0	1.2	5h	16.6	1.8
5b	12.5	1.3	5i	17.6	1.6
5c	17.8	3.2	5j	17.7	2.8
5d	4.7	0.0	5k	9.1	0.8
5e	15.2	1.8	5l	13.7	1.9
5f	14.0	1.5	5m	16.2	1.7
5g	10.3	0.1	5n	16.7	1.0
6a	7.9	0.3	6h	2.0	0.1
6b	8.8	0.2	6i	2.3	0.2
6c	6.7	0.1	6j	7.5	0.0
6d	3.2	0.0	6k	8.5	0.1
6e	4.5	0.0	6l	7.2	0.2
6f	7.0	0.2	6m	8.4	0.4
6g	2.7	0.1	7	16.0	2.6

^a $\Delta T_m = T_m (\text{DNA} + \text{ligand}) - T_m (\text{DNA})$. The concentrations of FPU22T and F10T were 0.4 μM , and the concentrations of compounds were 2.0 μM . The melting temperature of FPU22T in the absence of compounds was 46 $^{\circ}\text{C}$.

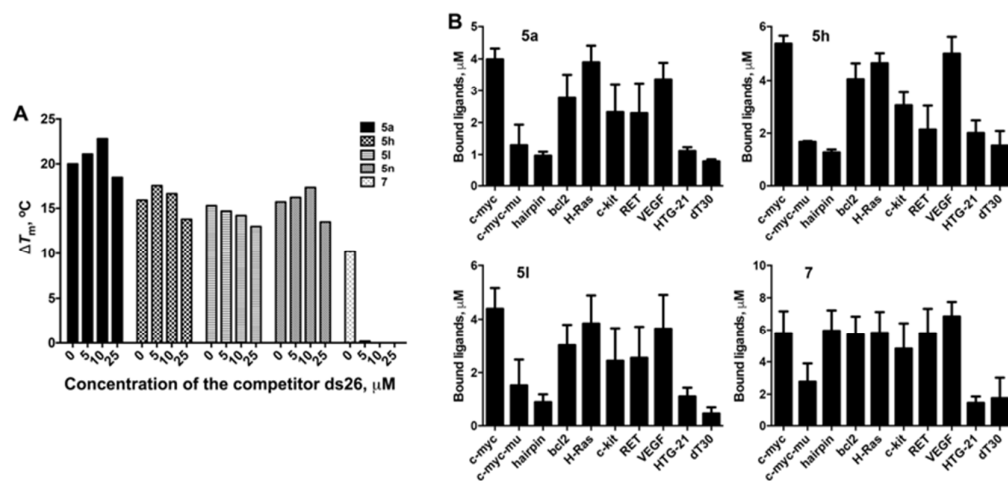


Figure 2. A. Competitive FRET results for T-BFQ derivatives **5a**, **5h**, **5l**, and **5n** without and with 5-fold (2 μM), 10-fold (4 μM) or 25-fold (10 μM) excess of duplex DNA competitor (ds26). The concentration of FPU22T was 0.4 μM . B. Competition dialysis results of T-BFQ derivatives **5a**, **5h**, and **5l**, and the reference compound **7** binding to the c-myc G-quadruplex or other DNA oligomers. A 10 mM Tris-HCl buffer (pH 7.4) containing 100 mM NaCl was used in the experiments.

Binding Affinities and Selectivity of T-BFQ Derivatives on c-myc G-quadruplex. In order to investigate the binding affinities of the T-BFQ derivatives with c-myc G-quadruplex, and their selectivity for quadruplex versus duplex DNA, the surface plasmon resonance (SPR) experiment was employed.³⁰ The binding constants (K_D values) for the binding of the T-BFQ derivatives to DNA were determined using SPR with biotinylated c-myc G-quadruplex DNA Pu22 and biotinylated duplex DNA (Table S1) attached to a streptavidin-coated sensor chip. As shown in Table 2, most of the T-BFQ derivatives could bind to the c-myc G-quadruplex more tightly than that to the duplex DNA, and the ratio of $K_D^{\text{duplex}}/K_D^{\text{Pu22}}$ ranged from 3.26 to 42.5. Among them, the most significant compound was **5n**, which possessed a binding selectivity of 42.5 folds ($K_D^{\text{duplex}}/K_D^{\text{Pu22}}$). At the

same time, the reference compound **7** showed similar binding affinities with both the quadruplex DNA and the duplex DNA (K_D^{Pu22} , 4.60 μM ; K_D^{duplex} , 4.46; $K_D^{\text{duplex}}/K_D^{\text{Pu22}}$ = 0.97). These results demonstrated that the incorporation of the 11-triazole containing side chains could give an improvement of the binding affinity and selectivity.

Table 2. Equilibrium binding constants (K_D) determined by SPR assay.

Cpd.	K_D (μM)		$K_D^{\text{duplex}}/K_D^{\text{Pu22}}$	Cpd.	K_D (μM)		$K_D^{\text{duplex}}/K_D^{\text{Pu22}}$
	Pu22	Duplex			Pu22	Duplex	
5a	2.43	18.0	7.41	5h	2.39	7.78	3.26
5b	3.05	53.4	17.5	5i	2.70	12.8	4.74
5c	3.46	14.0	2.36	5j	1.50	7.70	5.13
5d	3.65	30.5	8.36	5k	4.39	31.4	7.15
5e	3.85	36.6	9.48	5l	2.74	63.6	23.2
5f	3.78	31.2	8.25	5m	3.06	21.9	7.15
5g	2.38	35.3	14.8	5n	1.87	79.5	42.5
6a	2.84	21.6	7.6	6h	NA	NA	--
6b	1.75	25.6	14.6	6i	NA	NA	--
6c	NA ^a	NA	-- ^b	6j	NA	NA	--
6d	NA	NA	--	6k	7.33	NA	--
6e	NA	NA	--	6l	3.26	37.9	11.6
6f	2.51	NA	--	6m	0.94	8.83	9.39
6g	NA	NA	--	7	4.60	4.46	0.97

^a NA: not available between compound and DNA; ^b --: not comparable.

Similar SAR with the above data in FRET could still obtained in this section,

1
2
3 that most of the **T-BFQ** derivatives with positively charged amino substituents (series
4 **a**) could specifically and strongly bind to the *c-myc* G-quadruplex DNA, and
5 compounds with phenyl, alkyl, and glucosyl groups (**6c**, **6d**, **6e**, **6g**, **6h**, **6i**, and **6j**)
6 could barely bind to both the *c-myc* and duplex DNA. While the length of the side
7 chains could not show a significant effect on the K_D value.
8
9

10
11
12
13
14 Restricted by the measuring principle itself, the SPR experiment requires
15 immobilized nucleotide sequences on the sensor chip, which may affect the forming
16 and the structure of the G-quadruplex. Thus, alternative methods that could measure
17 in an absolute solution environment should be applied to give binding data. Here,
18 microscale thermophoresis (MST) was further applied since it is a sensitive method
19 for quantitative analysis of molecular interactions in solution at the microliter scale.³¹
20
21 Data in Table 3 exhibited consistency with those in the SPR assay. Firstly, most of the
22 **T-BFQ** derivatives with positively charged amino substituents (series **a**) could
23 specifically and strongly bind to the *c-myc* G-quadruplex DNA. The calculated K_D
24 values ranged from ($0.3 \pm 0.01 \mu\text{M}$ to $29.1 \pm 1.39 \mu\text{M}$). Among them, compound **5h**
25 showed strongest selectivity toward *c-myc* G-quadruplex ($K_D^{\text{duplex}}/K_D^{\text{Pu22}} = 35.0$).
26
27 Speaking of the reference compound **7**, it showed similar binding affinity and
28 selectivity with those in the SPR assay (K_D^{Pu22} , $3.36 \pm 0.24 \mu\text{M}$; K_D^{duplex} , 3.79 ± 0.09
29 μM ; $K_D^{\text{duplex}}/K_D^{\text{Pu22}} = 1.13$). Again, weak or not-detectable binding effects were
30 observed on the derivatives with phenyl, alkyl, and glucosyl groups (**6c**, **6d**, **6e**, **6f**,
31 and **6k**).
32
33
34
35
36
37
38
39
40
41
42
43
44
45
46
47
48

49
50 In addition, competition dialysis measurements were performed to further verify
51 the selectivity of the compound. The *c-myc* (Pu27) oligomer together with several
52 other oligomers (**Table S1**), including duplex DNA (hairpin), single strand (*c-myc*-mu
53 and dT30), and other G-quadruplex oligomers (bcl-2, H-Ras, c-kit, RET, VEGF, and
54
55
56
57
58
59
60

HTG-22) were placed in independent dialysis cassettes after the general annealing process. All the dialysis cassettes were submerged in a solution containing compounds and allowed to dialyze for 24 h. After spectrophotometric quantitation, the T-BFQs compound **5a**, **5h**, and **5l** were found to exhibit the highest binding with c-myc quadruplex, and weaker binding with other kinds of DNA structures (Figure 2B). As a reference, compound **7** showed similar binding affinity on c-myc and c-myc-mu or hairpin. Although we found the selectivity of the T-BFQs improved comparing with compound **7**, we need to clarify that this selectivity focused on the binding between c-myc quadruplex and duplex DNA. In fact, we could find that the T-BFQs still bind to other kinds of quadruplex DNAs, just like compound **7**.

Table 3. Calculated binding constants (K_D) determined by MST assay.

Cpd.	K_D (μM)		$K_D^{\text{duplex}}/K_D^{\text{Pu22}}$	Cpd.	K_D (μM)		$K_D^{\text{duplex}}/K_D^{\text{Pu22}}$
	Pu22	Duplex			Pu22	Duplex	
5a	2.3±0.19	50.7±2.18	22.0	5h	0.3±0.01	10.5±0.13	35.0
5b	1.8±0.12	24.7±0.66	13.7	5i	4.2±0.21	13.2±0.78	3.14
5c	29.1±1.39	10.1±0.588	0.35	5j	1.3±0.06	11.0±0.35	8.5
5d	2.4±0.09	54.7±2.10	22.8	5k	4.3±0.13	33.7±0.76	7.84
5e	1.8±0.15	31.2±0.55	17.3	5l	1.1±0.10	29.5±1.17	26.8
5f	6.3±0.44	113.0±3.34	17.9	5m	5.9±0.18	23.3±0.40	3.95
5g	3.1±0.12	35.2±0.63	11.4	5n	2.2±0.09	10.2±0.29	4.64
6a	2.8±0.08	12.6±0.93	4.5	6h	35.4±2.57	27.3±2.54	0.77
6b	2.1±0.12	3.4±0.13	1.6	6i	99.2±13.3264.0±6.71		2.66

6c	NA ^a	NA	-- ^b	6j	56.6±3.07398.0±7.42	7.03
6d	NA	NA	--	6k	NA	NA
6e	NA	NA	--	6l	6.4±0.30	12.5±0.97
6f	NA	NA	--	6m	5.5±0.45	30.0±2.74
6g	233.0±14.0	NA	--	7	3.36±0.24	3.79±0.09

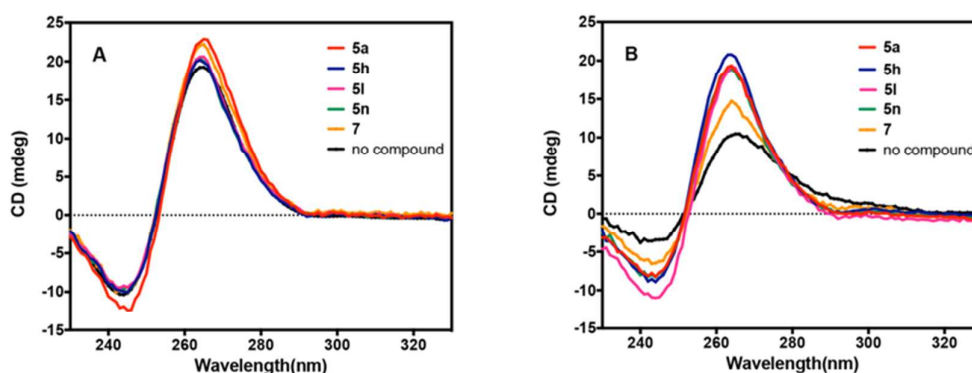
^a NA: not available between compound and DNA ; ^b --: not comparable

Interactions of the T-BFQ Derivatives on *c-myc* G-quadruplex. Basing on all the data from above assays, the **T-BFQ** derivatives with *in situ* protonated terminal substituents (amino groups and azo-heterocyclic rings) in series **a** remarkably increased their interactions with the *c-myc* G-quadruplex than the reference compound **7**. While the introduction of monohydroxyl, phenyl, alkyl, and glucosyl groups in series **b** could not interact well with the *c-myc* G-quadruplex. To comprehensively evaluate the interactions of these new synthesized **T-BFQ** derivatives, we selected compound **5a** (with the highest ΔT_m value), **5h** (sharing same end group with **5a**), **5n** (exhibited the highest selectivity in the SPR assay), and **5l** (exhibited the highest selectivity in the MST assay) for further studies.

Circular dichroism (CD) spectroscopy is usually used to determine the conformational of G-quadruplex DNA and the effects of ligands binding on quadruplex structures.³⁰ The oligomer Pu22 (Table S1) was used as the *c-myc* G-quadruplex forming sequence. The conformational properties of the Pu22 G-quadruplex DNA induced by the selected **T-BFQ** derivatives (**5a**, **5h**, **5l**, and **5n**) and the reference compound **7** were monitored by the CD spectroscopy. As is shown in Figure 3A, in the presence of 100 mM KCl, the Pu22 sequence showed a positive

1
2
3 peak at 262 nm and a negative peak at 242 nm, which suggested a typical parallel
4 G-quadruplex structure. Upon the addition of selected compounds to Pu22, no
5 significant change was observed while the peak height was slightly increased,
6 indicating that **T-BFQ** could still maintain parallel *c-myc* G-quadruplex conformation
7 in the presence of potassium ion.
8
9

10
11
12
13
14 The CD spectroscopy of Pu22 in the absence of metal ion was also studied. As
15 shown in Figure 3B, similar with the CD spectrum of Pu22 in the presence of KCl,
16 the CD spectrum of Pu22 exhibited a negative peak at 240 nm and a positive peak at
17 260 nm. The positive peak at 260 nm and the negative peak at 240 nm were
18 drastically increased after the treatment with **T-BFQ** derivatives. In addition, more
19 significant changes were observed upon the addition of the **T-BFQ** derivatives than
20 the reference compound **7**. All these CD studies illustrated that tested compounds
21 could effectively induce the formation of parallel *c-myc* G-quadruplex conformation
22 in the absence of metal cations, which further indicated a strong interaction between
23 the ligands and G-quadruplex DNA.
24
25
26
27
28
29
30
31
32
33
34
35
36



37
38
39
40
41
42
43
44
45
46
47
48
49
50 **Figure 3.** CD spectra of Pu22 (5 μ M) in 10 mM Tris-HCl buffer (pH 7.4) in the
51 presence of 100 mM KCl (A), and in the absence of KCl (B). CD spectra of Pu22
52 (black line), and Pu22 in the presence of 5 μ M of **5a**, **5h**, **5l**, **5n**, and **7**, respectively.
53
54
55
56
57
58
59
60

Effects of the T-BFQ Derivatives on the Proliferation of Tumor Cells.

To investigate the antitumor activity of the derivatives, MTT assay was employed to evaluate the cytotoxicity of all the T-BFQ derivatives against human lymphoma cell lines Raji and CA46, and lung adenocarcinoma cell line A549, as well as primary cultured mouse mesangial cell line (in which the proliferation does not depend on *c-myc* expression). The cytotoxicity of the T-BFQ derivatives were shown as IC₅₀ values (concentration for 50% inhibition) in Table 4. As for the control, the reference compound **7** showed strong cytotoxicity in all cells, including tumor cells and normal cells. Most compounds in series **a** showed diverse cytotoxicity between tumor cells and normal cells, indicating the specificity of these compounds were improved. Among them, compound **5a**, **5c**, **5e**, **5f**, **5h**, **5j**, **5l**, and **5m**, showed strong cytotoxicity against Raji, A549, and CA46 cells, while weak cytotoxicity against primary cultured mouse mesangial cells. However, most compounds had weak cytotoxicity in all cells, such as compound **6j** and **6l**. Although with a few exceptions, the structure-activity relationship in MTT assays was basically consistent with that found in *in vitro* assays.

Table 4. IC₅₀ values (μM) of derivatives against tumor cells and the primary cultured mouse mesangial cell.

Cpd.	Raji	A549	CA46	Mesangial cells	Cpd.	Raji	A549	CA46	Mesangial cells
5a	5.53	3.83	1.06	21.87	5h	3.06	3.18	0.05	15.74
5b	10.28	13.38	0.54	48.03	5i	0.19	10.5	0.38	18.32
5c	0.10	2.80	2.28	10.75	5j	0.27	3.73	1.30	12.06
5d	15.79	>50	22.02	>50	5k	18.00	20.64	12.76	16.58

5e	2.93	5.27	2.74	19.53	5l	3.96	0.26	0.02	16.05
5f	2.73	5.11	5.60	19.84	5m	4.91	5.15	0.17	30.45
5g	27.40	0.53	3.01	25.24	5n	13.90	12.75	1.50	20.81
6a	15.29	21.86	7.55	28.27	6h	3.70	9.75	6.15	41.27
6b	28.79	19.42	11.53	47.94	6i	5.60	12.12	10.64	42.18
6c	5.10	>50	13.85	>50	6j	>50	>50	>50	>50
6d	4.67	25.08	15.12	16.25	6k	22.16	25.30	9.73	34.92
6e	11.62	>50	14.75	>50	6l	>50	>50	46.09	>50
6f	33.64	19.16	14.02	>50	6m	43.09	>50	>50	>50
6g	41.67	17.76	14.10	>50	7	0.05	2.11	0.01	5.51

To precisely identify the effects of the **T-BFQ** derivatives on cell's proliferation, we took the real time cellular analysis (RTCA) assays using compound **5a**, **5h**, **5l**, **5n**, and the reference compound **7**. A549 cells (with overexpression of *c-myc*) and primary cultured mouse mesangial cells (the proliferation does not depend on *c-myc* expression) were treated with various concentrations of compounds (0 μM , 1/8 IC_{50} , 1/2 IC_{50} , and IC_{50}) in RTCA for 100 h.

The cell proliferation results of **5a** and **7** were shown in Figure 4 (results of **5h**, **5l**, and **5n** were shown in Figure S3). Compound **5a** showed significant growth arrest on A549 cells at the concentration of 5 μM , while no effect on primary cultured mouse mesangial cells. To be noted, the inhibitory activity of **7** on A549 cells was stronger than **5a**, while the inhibitory activity could also be observed on normal cells at high concentration. Similar data could be detected in **5h**, **5l**, and **5n** (Figure S3). These results were consistent with the MTT results that the derivatives had relatively

selectivity on tumor cells over normal cells, which might come from their specificity of *c-myc* gene. To exclude the possibility that differential effects of the compounds come from cellular uptake efficiency, we also performed the cellular uptake experiments. The uptake amounts of compounds in the mesangial cells were higher than those in A549 cells (Figure S4), indicating that compounds exhibited lower cytotoxicity on the mesangial cells wasn't due to cellular uptake.

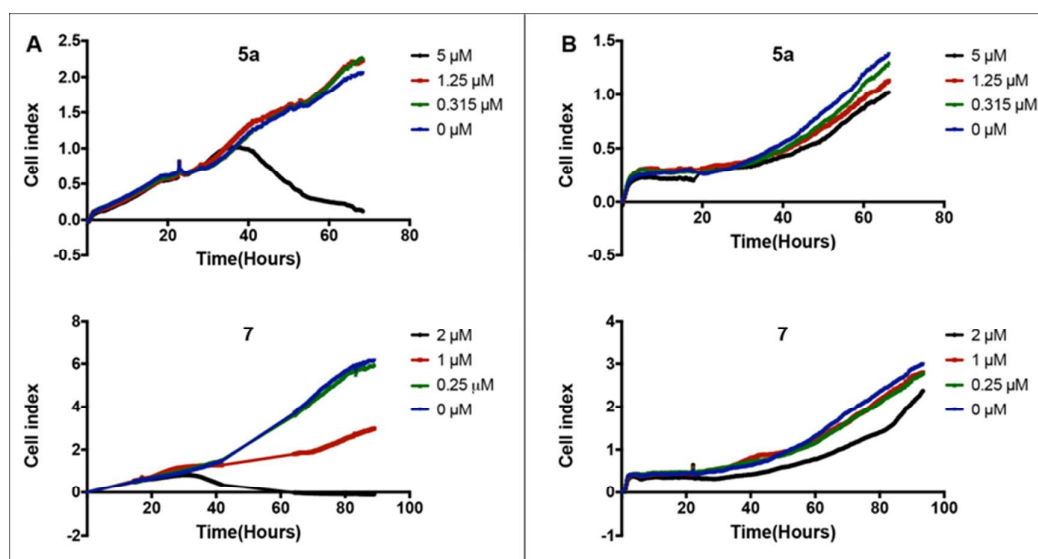


Figure 4. The effect of compound **5a** and **7** on the proliferation of A549 cells (A) and primary cultured mouse mesangial cells (B) measuring by using RTCA assay. A549 lung adenocarcinoma cells and primary cultured mouse mesangial cells were seeded (2000 cells each well) on E-Plate 16 PET culturing about 20 h before compound treatment. Cells were treated with various concentrations of **5a**, **7**, or DMSO control.

Down-Regulation of *c-myc* Transcription via Specific Interaction with the G-Quadruplex Forming Sequence in the Promoter. To investigate whether the derivatives could affect the *c-myc* transcription, dual-luciferase reporter assay, reverse-transcription-polymerase chain reaction (RT-PCR), and Western blot assay were firstly applied. Dual-luciferase reporter assays were used with a psicheck2

1
2
3 plasmid carrying the *c-myc* promoter in front of the *Renilla* luciferase (Figure 5A),
4
5 and the same plasmid carrying *Firefly* luciferase downstream. After transfection, Raji
6
7 cells were treated with the **T-BFQ** derivatives (at 1/2 IC₅₀) for 48 h. As shown in
8
9 Figure 5B, the ratio of *Renilla*/*Firefly* luciferase with the *c-myc* promoter decreased.
10
11 Most derivatives could cause more obvious decrease in the ratio than the reference
12
13 compound **7**. To be noted, the structure-activity relationship found in *in vitro*
14
15 experiments, that compounds containing an amino groups or an azoheterocyclic ring
16
17 showed stronger activities, could not be found in the dual luciferase reporter assay. All
18
19 derivatives showed similar inhibitory activities on luciferase transcription. The
20
21 possible reason might be the complicated mechanism of other compounds in cells.
22
23

24
25 To identify whether this inhibitory activity was due to the interaction with the
26
27 G-quadruplex, we further constructed plasmid carrying the mutant *c-myc* promoter
28
29 which could not form a G-quadruplex structure. Four compounds, **5a**, **5h**, **5l**, and **7**
30
31 possessing relative strong activities in all the above assays, were used in this assay. As
32
33 shown in Figure 5C, these compounds showed significant inhibitory activities on
34
35 wild-type plasmid, while no significant effects on mutant plasmid.
36
37
38
39
40
41
42
43
44
45
46
47
48
49
50
51
52
53
54
55
56
57
58
59
60

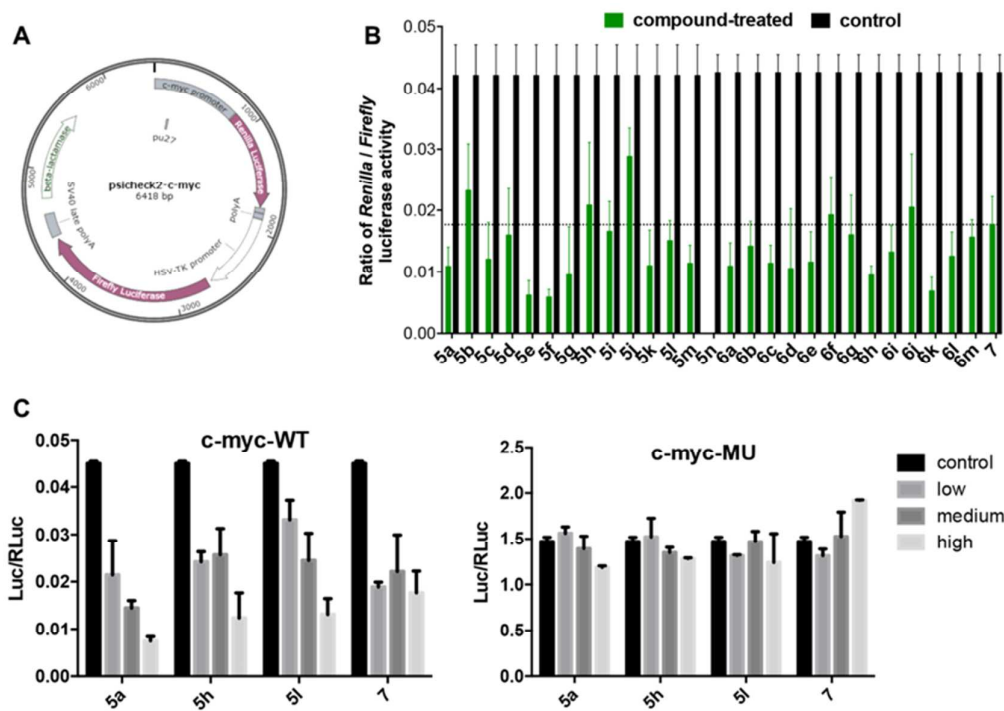
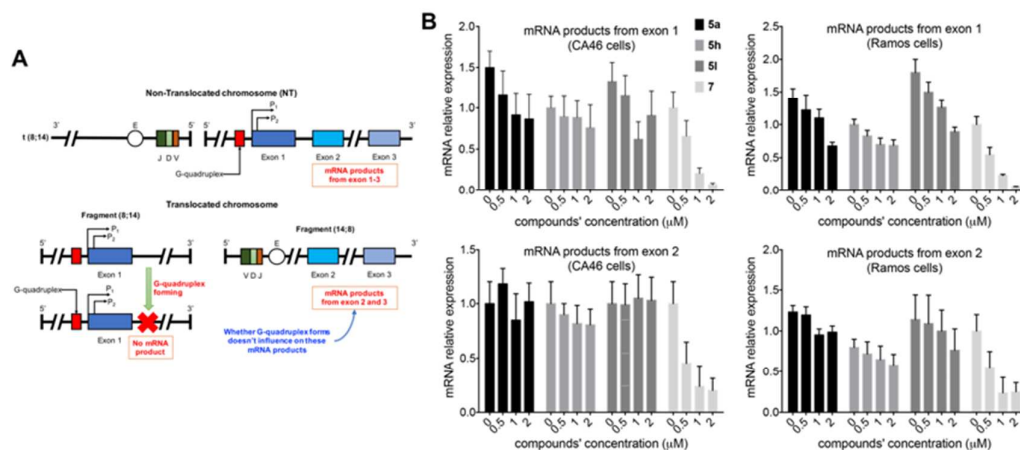


Figure 5. The effects of T-BFQ derivatives on *c-myc* promoter's activity via dual luciferase reporter assays. (A) Schematic diagram of the plasmids used in dual luciferase reporter assays. The psiCHECK2 plasmid carrying the *c-myc* promoter in front of the *Renilla* luciferase, and the *Firefly* luciferase in the same plasmid, was transfected into cells. (B) Column graph showing the relative expression level of the *Renilla* luciferase (activity of *Renilla* luciferase/activity of *Firefly* luciferase) after the addition of T-BFQ derivatives. All the experiments were repeated for three times. (C) Column graph showing the relative expression level of the *Renilla* luciferase (activity of *Renilla* luciferase/activity of *Firefly* luciferase) in plasmids containing wild-type or mutant constructs after the addition of T-BFQ derivatives. Cells were treated with 1/8 IC₅₀ (low), 1/2 IC₅₀ (medium), and IC₅₀ (high) of compounds. All the experiments were repeated for three times.

To further identify whether this down-regulation was happened through **T-BFQ** derivatives' interactions with the *c-myc* G-quadruplex-forming sequence, an exon specific experiment was carried out. The translocation between chromosomes 8 and 14 in Burkitt's lymphoma CA46 cell can produce varying MYC mRNAs. G-quadruplex-forming sequence can only exist in the fragment (8;14) of non-translocated chromosome (NT), but not in the fragment (14;8) in translocated CA46 cells. Therefore, the NT products (mRNA products from exon 1-3) are normal, with a functional MYC under the control of a G-quadruplex; whereas the functional MYC produced from the fragment (14;8) (mRNA products from exon 2 and 3) on the T allele lacks G-quadruplex-mediated control. Using primers specific to two different exons, the exon 1 and exon 2 mRNA products, respectively, of the CA46 cell line can be examined independently (Figure 6A).³²⁻³³ As shown in Figure 6B, the amplification of exon 1 in CA46 and Ramos cells were decreased upon addition of three compounds, **5a**, **5h**, and **5i**, respectively; while no significant changes were observed in the amplification of exon 2 in these two cells. As for the control, the reference **7** could decrease mRNA products for both the exon 1 and exon 2 in these two cells. These results gave further evidence that the specificity of the new **T-BFQ** derivatives were improved.



1
2
3 **Figure 6.** Effects of T-BFQ derivatives on *c-myc*'s translocation. (A) Exon-specific
4 expression in Raji cells based on translocation events. (B) Real-time RT-PCR results
5 of Exon-specific expression in CA46 and Ramos cells upon addition of compound **5a**,
6 **5h**, **5l**, and **7** with concentrations from 0 to 2 μ M. mRNA relative expression was
7 calculated with ct values and columned in graph. All the experiments were repeated
8 for three times.
9
10
11
12
13
14
15
16
17

18 Furthermore, we explored the effects of **5a**, **5h** and **5l** on the mRNA level of
19 *c-myc*, and subsequent the protein level. In Figure 7A, the results of RT-PCR revealed
20 that **5a**, **5h** and **5l** reduced the mRNA level of *c-myc* in a dose-dependent manner but
21 didn't affect the mRNA level of *β -actin*. These results suggested that the compounds
22 **5a**, **5h** and **5l** could suppress the transcription of *c-myc* and subsequently suppress the
23 translation of this gene (Figure 7B).
24
25
26
27
28
29
30
31

32 The overall evaluation results of exon specific experiment, RT-PCR and western
33 blot suggested that compound **5a**, **5h** and **5l**, as stabilizer to *c-myc* G-quadruplex,
34 could specifically interact with *c-myc* G-quadruplex-forming sequence and hence
35 down-regulate *c-myc* transcription in cancer cells.
36
37
38
39

40 To make a clear map of compounds' selectivity in cell, we further evaluated the
41 transcription level of some other oncogenes (Figure S5), including
42 G-quadruplex-related genes PDGFA, RET, c-kit, k-Ras, and bcl-2, and other
43 oncogenes without G-quadruplex-forming sequences (GLI1 and AML). It turned out
44 that the compounds didn't show significant effects on most of these genes'
45 transcription. Moreover, we constructed dual-luciferase plasmids carrying different
46 G-quadruplex-forming genes' promoters (including bcl-2, RET, c-kit, and VEGF).
47 After detection of the luciferase expression, we found that these compounds had little
48
49
50
51
52
53
54
55
56
57
58
59
60

effects on these gene's promoter activity (Figure S6).

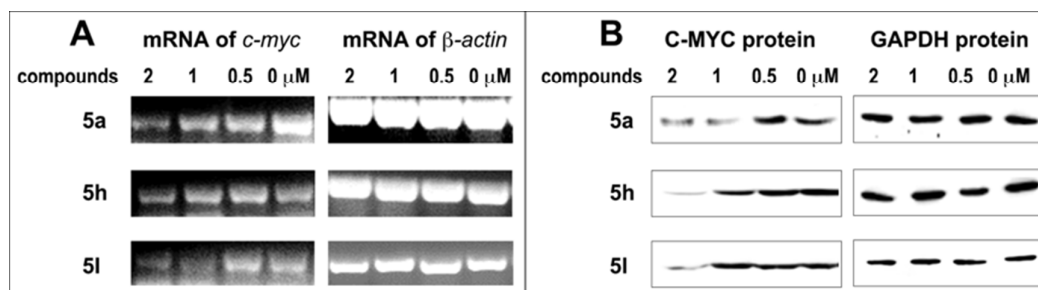


Figure 7. The Effects of **5a**, **5h** and **5l** on *c-myc* transcription and expression after 6-h treatment in Raji cells. (A) The transcription level of *c-myc* gene in the presence of **5a**, **5h** and **5l** in Raji cells by using RT-PCR. β -actin was used as an internal control. All the experiments were repeated for three times. (C) Expression level of C-MYC protein under the treatment of increased concentrations of **5a**, **5h** and **5l** in Raji cells by using Western blot. β -Actin was used as an internal control. All the experiments were repeated for three times.

G₀/G₁ Phase Arrest of Raji Cells by T-BFQ Derivatives. Since *c-myc* is an important oncogene and is closely related with the cell cycle regulation, the three compounds were further evaluated their effects on cell cycle of Raji cells by flow cytometric assay which enables quantification of the total cellular population in different phases of the cell cycle (G₀/G₁, S, and G₂/M). These compounds showed similar effects on cell cycle of Raji cells, which arrested cells in the G₀/G₁ phase with an increase about 15% upon treatments with compounds at 1 μ M concentration for 6 h (Figure 8). Specifically, the representative compound **5a** increased cells in the G₀/G₁ phase from 32.6% to 48.4%, and correspondingly decrease cell population in the G₂/M phase.

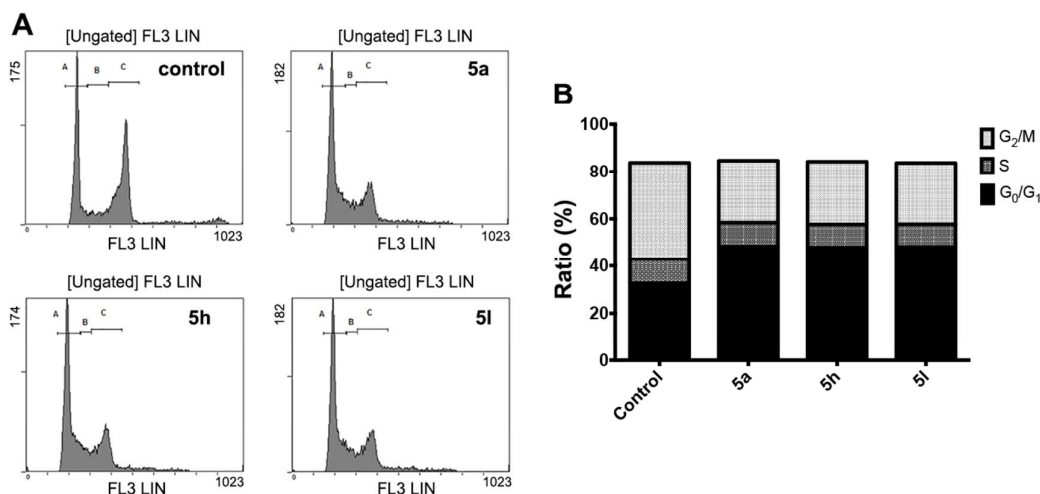


Figure 8. The induction of G₀/G₁ phase arrest in Raji cells by compounds **5a**, **5h** and **5l**. (A) Cell cycle analysis after propidium iodide (PI) staining after 6-h treatment with 1 μM **5a**, **5h**, and **5l**, or 0.1% DMSO in Raji cells. (B) The percentage of cells in different phases of the cell cycle, analyzed by EXPO32 ADC software. All the experiments were repeated for three times.

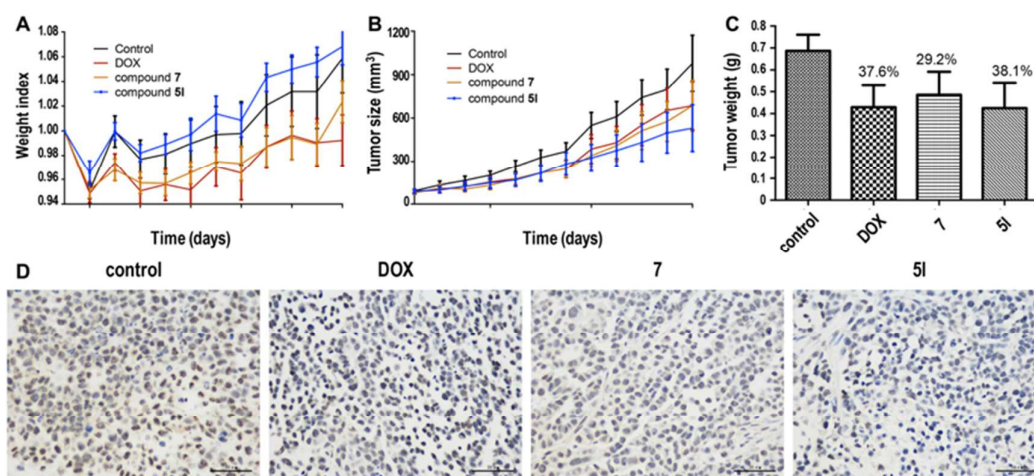
T-BFQs Inhibit Tumor Growth in a Human Lung Cancer Xenograft.

Considering the importance of c-Myc for tumor growth, we evaluated compound **5l**'s antitumor activity *in vivo*. Firstly, a colony formation assay was performed to evaluate whether the T-BFQ compounds reduced the tumorigenicity and vitality of A549 cells. As shown in Figure S7, after treated with **5a**, **5h**, **5l**, and **7** for 8 days, colony formation obviously decreased.

In addition, the *in vivo* anti-tumor activities against a human lung cancer xenograft (A549) in athymic nude mice was evaluated. The results were presented in Figure 9. An experimental group of ten tumor-bearing mice was treated with compound **5l** once a day for 12 days at a dose of 6.25 mg/Kg. No significant change in body weight was observed during the treatment (Figure 9A). The negative control

1
2
3 group, which was treated with saline only, had an average tumor volume $>900 \text{ mm}^3$
4
5 after 12 days (Figure 9B). In contrast, the tumor-bearing mice treated with compound
6
7 **5I** had an average tumor volume of $< 400 \text{ mm}^3$ and had an inhibition rate of 38.1%
8
9 (Figure 9C). The dose of reference compound **7** was 7.5 mg/Kg; this treatment
10
11 obtained an anti-tumor effect with an inhibition rate of 29.2%, which was slightly
12
13 lower than that of compound **5I**. The positive control group was treated once two days
14
15 with doxorubicin at a dose of 1 mg/kg for 12 days and showed an effect similar to that
16
17 of compound **5I** with an inhibition rate of 37.6%.

21 To determine whether the expression of c-Myc was consistently affected within
22
23 tumors by treatment with compound **5I** and **7**, we assessed the c-Myc (brown area in
24
25 Figure 9D) in tumor tissue using immunohistochemistry (IHC). The experimental
26
27 group exhibited significantly decreased expression relative to the negative control
28
29 group. The results indicated c-Myc down-regulation by compound **5I** and **7** might
30
31 contribute to tumor inhibition *in vivo*.



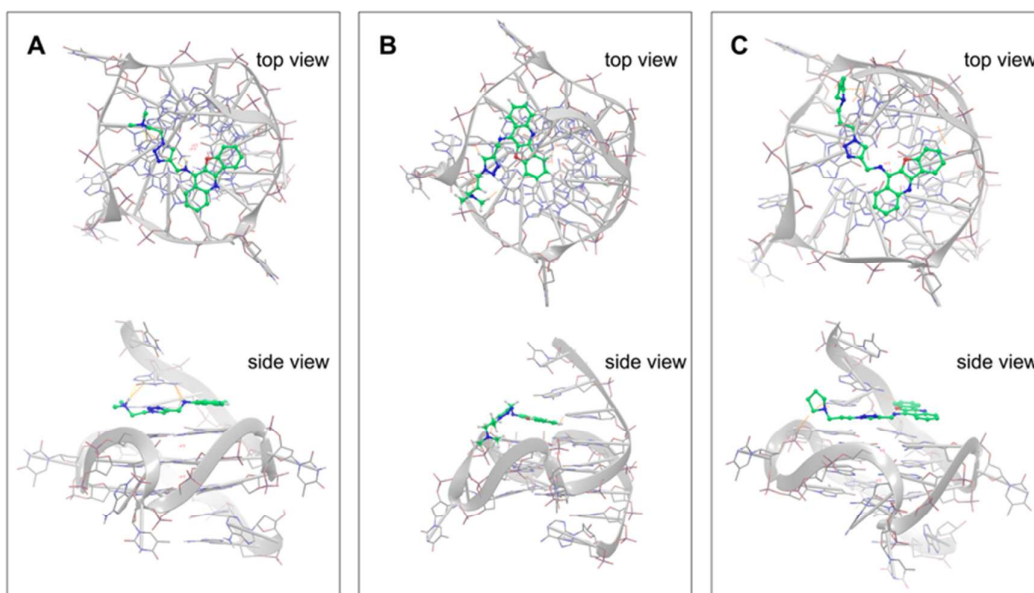
34
35
36
37
38
39
40
41
42
43
44
45
46
47
48
49
50
51
52 **Figure 9.** Compound **5I** and **7**, doxorubicin, and saline were administered by i.p.
53
54 injection to athymic nude mice with human tumor xenografts established using A549
55
56 lung cancer cells. The mice were injected i.p. once a day for 12 days. The control
57
58 group was injected with 150 μL of saline. The positive control group (DOX) received
59
60

1
2
3 doxorubicin by i.p. injection at a dose of 1 mg/Kg, once two days for 12 days.
4
5 Compound **5l** and **7** were similarly administered to mice, once a day, at a dose of 6.25
6
7 mg/Kg, and 7.5 mg/Kg, respectively. The body weight (A) and tumor volume (B)
8
9 were recorded every two days, and the tumor weight was evaluated when the
10
11 treatment ended (C). The inhibition rate was calculated using (tumor weight in
12
13 drug-treatment group) / (tumor weight in control group) and indicated on the column.
14
15 (D) The expression of c-Myc protein was identified by IHC, and pictures were taken
16
17 at 400 × magnification. Images of three independent samples in each group were
18
19 selected and presented for to give an overall illustration of the results.
20
21
22
23
24

25 **Binding Mode Exploration by Using Molecular Modeling.** Molecular
26
27 docking was performed to provide a possible binding mode of compound **5h** and **5l**
28
29 with the *c-myc* G-quadruplex. The ligands were docked to the three-dimensional
30
31 structures of *c-myc* G-quadruplex (PDB code: 2L7V, authors will release the atomic
32
33 coordinates and experimental data upon article publication) determined by solution
34
35 state NMR spectroscopy as mentioned in the introduction. The docking results of **5a**,
36
37 **5h** and **5l** to *c-myc* G-quadruplex with highest scores were shown in Figure 10A. The
38
39 docking results of **5h** showed that the benzofuroquinoline scaffold could effectively
40
41 stack on the external 5'-terminal G-quartet, and the triazole containing side chain
42
43 were properly oriented and directed into the DNA grooves and fill the groove space,
44
45 which helped lock the ligand onto the *c-myc* G-quadruplex. Specifically, the triazole
46
47 moiety interact with the loop through H-bond. The positively charged terminal group
48
49 was well accommodated in the groove towards the negatively charged phosphate
50
51 diester backbone, and formed electrostatic interactions and H-bonds. In addition, by
52
53 comparing with the compound **5a** and **5h**, compounds with longer side chain gain
54
55
56
57
58
59
60

1
2
3 better score (-9.137) than that with shorter side chain (-7.696), again, indicating that
4
5 longer side chains might have better interactions with the groove.
6

7 Result of **5l** demonstrated a similar binding mode to the *c-myc* G-quadruplex.
8
9 However, the orientation of the side chain was slightly different from the above two
10
11 compounds. The triazole moiety seemed to possess a π - π stacking interaction with one
12
13 of the guanines in the G-quartet. These results further reinforced our design idea that
14
15 the triazole might interact with the G-quadruplex.
16
17



18
19
20
21
22
23
24
25
26
27
28
29
30
31
32
33
34
35
36
37
38
39
40
41 **Figure 10.** Docking results of derivatives **5a** (A), **5h** (B), and **5l** (C) onto the *c-myc*
42
43 G-quadruplex (top views onto the 5' of the *c-myc* G-quadruplex and side views, PDB
44
45 code: 2L7V, authors will release the atomic coordinates and experimental data upon
46
47 article publication).
48

51 52 Conclusions

53
54 A series of derivatives with the incorporation of 1,4-triazole moiety by using
55
56 click chemistry have been designed, synthesized and evaluated as effective and
57
58
59
60

1
2
3 selective *c-myc* G-quadruplex binding ligands. Results of FRET, SPR and MST
4
5 experiments suggested that positive charged terminal substituents played a crucial role
6
7 in the stabilization ability, binding affinity and the selectivity of the derivatives. It is
8
9 noteworthy that the introduction of 1,4-triazole moiety lead to positive impact on the
10
11 binding affinity of the ligands. In addition, derivatives with longer side chains (n=3)
12
13 possessed better activity to the *c-myc* G-quadruplex. In line with the *in vitro* assays,
14
15 subsequent bioassays demonstrated that the selected derivatives **5a**, **5h**, and **5l**
16
17 specifically down-regulated *c-myc* gene transcription and expression in Raji cells,
18
19 presumably through the stabilization of *c-myc* G-quadruplex structure. Results from
20
21 the flow cytometric assays suggested that **5a**, **5h**, and **5l** could arrest Raji cell cycle in
22
23 G₀/G₁. In addition, RTCA assays indicated that these derivatives could remarkably
24
25 inhibited A549 cell proliferation, without influencing normal primary cultured mouse
26
27 mesangial cells. Altogether, the reported results proved that modification by using
28
29 click chemistry is an efficient approach for obtaining potent and selective *c-myc*
30
31 promoter G-quadruplex binding ligands.
32
33
34
35

36 To be noted, the activities of these new derivatives actually were similar with
37
38 that of the reference compound **7**. Good transcriptional inhibition activity but poor
39
40 selectivity in compound **7** indicated that this compound might have alternative targets
41
42 *in vivo*. On the other hand, we have to emphasize one thing that the improved
43
44 selectivity in the present study refers to the binding selectivity of T-BFQs on *c-myc*
45
46 quadruplex against that on duplex DNA. The specificity of these compounds to a
47
48 certain G-quadruplex (such as *c-myc*) versus other quadruplex genes is still need to
49
50 further improvement.
51
52
53
54
55

56 ■ Experimental section

57
58
59
60

1
2
3 **General Methods in Synthesis.** All chemicals were purchased from
4 commercial sources unless otherwise specified. All chemical structures were
5 confirmed by ^1H and ^{13}C NMR spectra and HRMS spectrometry. ^1H and ^{13}C NMR
6 spectra were recorded using TMS as the internal standard in $\text{DMSO-}d_6$, CD_3OD or
7 CDCl_3 with a Bruker BioSpin GmbH spectrometer at 400 MHz and 100 MHz,
8 respectively. High-resolution mass spectra were obtained with a MAT95XP (Thermo)
9 mass spectrometer. Melting points (mp) were determined using an SRS-OptiMelt
10 automated melting point instrument without correction. The purity of the synthesized
11 compound was confirmed to be higher than 95% by using analytical HPLC performed
12 with a dual pump Shimadzu LC-20 AB system equipped with an Ultimate XB-C18
13 column (4.6×250 mm, $5 \mu\text{m}$) and eluted with methanol-water (30:70-65:35)
14 containing 0.1% TFA at a flow rate of 1.0 mL/min.
15
16
17
18
19
20
21
22
23
24
25
26
27
28
29
30
31

32 **Synthesis of the intermediate *N*-(prop-2-yn-1-yl)**
33 **benzofuro[3,2-*b*]quinolin-11-amine (2).** Compound **2** was synthesized from the
34 key intermediate 11-chlorobenzofuro[3,2-*b*]quinoline (**1**) that was prepared followed
35 a literature procedure.²¹ To gain compound **2**, pTsOH (2.28 g, 12 mmol) was heated at
36 120°C for 10 min in a 15 mL seal tube. Compound **1** (1.01 g, 4 mmol) was added to
37 the liquefied pTsOH and stirred for 10 min. The mixture was allowed to cool to room
38 temperature and then 2-propynylamine (0.44 g, 8 mmol) was added. The mixture was
39 heated and stirred at 120°C for 6 h. Then, the mixture was allowed to cool to room
40 temperature and 10 mL methanol and 25 mL CHCl_3 was added to dissolve the residue.
41 10 mL of 1 N NaOH solution was added to adjust pH value to 12. Then the combined
42 organic phase was washed with saturated NaCl solution and water, and dried over
43 anhydrous Na_2SO_4 . After concentration, the product was purified by column
44
45
46
47
48
49
50
51
52
53
54
55
56
57
58
59
60

1
2
3 chromatography on silica gel with CH₂Cl₂/MeOH/NH₃·H₂O (250:1:0.1-100:1:0.1) as
4
5 eluent. Yield 72%; m.p.216.0-217.2 °C; ¹H NMR (400 MHz, CDCl₃) δ 8.35 (d, *J* = 7.7
6
7 Hz, 1H), 8.21 (d, *J* = 8.5 Hz, 1H), 7.90 (d, *J* = 8.5 Hz, 1H), 7.66 (t, *J* = 7.6 Hz, 1H),
8
9
10 7.62 – 7.55 (m, 2H), 7.44 (dt, *J* = 14.0, 6.7 Hz, 2H), 5.22 (s, 1H), 4.83 (dd, *J* = 5.8,
11
12 2.3 Hz, 2H), 2.31 (t, *J* = 1.9 Hz, 1H). ¹³C NMR (101 MHz, CDCl₃) δ 158.3, 147.4,
13
14 146.8, 134.1, 132.9, 130.1, 129.7, 127.9, 124.2, 123.2, 123.2, 122.1, 120.0, 118.2,
15
16 112.0, 80.8, 72.5, 35.6. HRMS (ESI) *m/z*: calcd for C₁₈H₁₂N₂O, [M+H]⁺ 273.1022,
17
18 found 273.1022.
19
20
21
22

23 **General Procedure for the Preparation of the 11-Triazole Substituted**
24 **Benzofuro[3,2-*b*]Quinolone (5a-5n and 6a-6m) via Click Reaction. 2**

25 (0.272g, 1 mmol) was dissolved in a 2:1 mixture of THF/H₂O (10 mL). Solution of
26
27 CuSO₄·5H₂O (100 μL, 100 mM) and sodium ascorbate (300 μL, 100 mM) were
28
29 added and the mixture stirred for 1 min. The respective azides **3a-3n** or **4a-4m** (3
30
31 mole equivalent) was added and the solution was allowed to stir for 6-12 h under
32
33 35 °C, and the reaction was monitored intermittently by TLC. The reaction mixture
34
35 was finally concentrated in vacuum and the products were purified by column
36
37 chromatography on silica gel with CH₂Cl₂/MeOH/NH₃·H₂O (80:1:0.1-20:1:0.1) as
38
39 eluent to afford the proposed compounds in 55-92% yield.
40
41
42
43
44

45 *N*-((1-(2-(dimethylamino)ethyl)-1*H*-1,2,3-triazol-4-yl)methyl)benzofuro[3,2-*b*]
46
47 *quinolin-11-amine* (**5a**). Compound **2** was treated with **3a** according to general
48
49 procedure to afford **5a** as a pale yellow solid. 88% yield. ¹H NMR (400 MHz, CDCl₃)
50
51 δ 8.41 (d, *J* = 7.7 Hz, 1H), 8.18 (dd, *J* = 8.5, 0.7 Hz, 1H), 7.94 (d, *J* = 8.5 Hz, 1H),
52
53 7.71 (s, 1H), 7.66-7.58 (m, 3H), 7.43 (m, 2H), 5.94 (s, 1H), 5.36 (d, *J* = 5.8 Hz, 2H),
54
55 4.38 (t, *J* = 6.2 Hz, 2H), 2.69 (t, *J* = 6.2 Hz, 2H), 2.19-2.14 (s, 6H). ¹³C NMR (101
56
57
58
59
60

1
2
3 MHz, CDCl₃) δ 158.1, 147.1, 146.9, 145.5, 133.7, 130.0, 129.5, 128.0, 124.0, 123.5,
4
5 123.2, 122.5, 122.2, 120.4, 118.2, 111.8, 58.6, 48.1, 45.2, 41.0. HPLC purity: 99.8%.
6
7 HRMS (ESI) m/z : calcd for C₂₂H₂₂N₆O, [M+H]⁺, 387.1928 found 387.1915.
8

9
10 *N*-((1-(2-(diethylamino)ethyl)-1*H*-1,2,3-triazol-4-yl)methyl)benzofuro[3,2-*b*]
11 *quinolin-11-amine* (**5b**). Compound **2** was treated with **3b** according to general
12 procedure to afford **5b** as a pale yellow solid. 83% yield. m.p. 133.1-134.3 °C; ¹H
13 NMR (400 MHz, CDCl₃) δ 8.39 (d, J = 6.9 Hz, 1H), 8.19 (d, J = 8.4 Hz, 1H), 7.93 (d,
14 J = 8.5 Hz, 1H), 7.63 (dt, J = 19.1, 7.5 Hz, 4H), 7.45 (t, J = 7.3 Hz, 2H), 5.81 (s, 1H),
15 5.36 (d, J = 5.8 Hz, 2H), 4.33 (s, 2H), 2.78 (s, 2H), 2.40 (d, J = 6.9 Hz, 4H), 0.79 (t, J
16 = 6.9 Hz, 6H). ¹³C NMR (101 MHz, CDCl₃) δ 158.1, 146.9, 146.7, 145.3, 133.8, 133.7,
17 130.1, 129.4, 128.1, 124.1, 123.3, 123.2, 122.8, 122.2, 120.4, 118.1, 111.8, 52.7, 49.0,
18 47.1, 40.9, 11.7. HPLC purity: 99.2%. HRMS (ESI) m/z : calcd for C₂₄H₂₆N₆O,
19 [M+H]⁺, 415.2241 found 415.2246.
20
21
22
23
24
25
26
27
28
29
30
31

32 *N*-((1-(2-aminoethyl)-1*H*-1,2,3-triazol-4-yl)methyl)benzofuro[3,2-*b*]quinolin-11-
33 *amine* (**5c**). Compound **2** was treated with **3c** according to general procedure to afford
34 **5c** as a pale yellow solid. 72% yield. m.p. 130.4-131.5 °C; ¹H NMR (400 MHz, CDCl₃)
35 δ 8.36 (d, J = 7.6 Hz, 1H), 8.17 (d, J = 8.4 Hz, 1H), 7.93 (d, J = 8.4 Hz, 1H),
36 7.68-7.55 (m, 4H), 7.44 (t, J = 7.6 Hz, 2H), 5.83 (t, J = 5.9 Hz, 1H), 5.34 (d, J = 6.1
37 Hz, 2H), 4.36-4.27 (m, 2H), 3.20-3.08 (m, 2H). ¹³C NMR (101 MHz, DMSO-*d*₆) δ
38 157.9, 147.2, 146.6, 146.4, 135.2, 133.2, 130.7, 129.4, 128.4, 123.8, 123.7, 123.6,
39 123.5, 122.8, 122.0, 118.6, 112.7, 53.0, 42.4, 40.5. HPLC purity: 99.9%. HRMS (ESI)
40 m/z : calcd for C₂₀H₁₈N₆O, [M+H]⁺, 359.1615 found 359.1620.
41
42
43
44
45
46
47
48
49
50
51

52 *N*-((1-(2-morpholinoethyl)-1*H*-1,2,3-triazol-4-yl)methyl)benzofuro[3,2-*b*]
53 *quinolin-11-amine* (**5d**). Compound **2** was treated with **3d** according to general
54 procedure to afford **5d** as a white solid. 92% yield. m.p. 209.1-210.8 °C; ¹H NMR
55
56
57
58
59
60

1
2
3 (400 MHz, CDCl₃) δ 8.37 (d, $J = 7.5$ Hz, 1H), 8.18 (dd, $J = 8.5, 0.9$ Hz, 1H), 7.93 (d,
4
5 $J = 8.0$ Hz, 1H), 7.69-7.64 (m, 1H), 7.63-7.57 (m, 3H), 7.48-7.43 (m, 2H), 5.76 (t, $J =$
6
7 6.3 Hz, 1H), 5.35 (d, $J = 6.3$ Hz, 2H), 4.37 (t, $J = 6.1$ Hz, 2H), 3.50-3.43 (m, 4H),
8
9 2.71 (t, $J = 6.1$ Hz, 2H), 2.39-2.29 (m, 4H). ¹³C NMR (101 MHz, CDCl₃) δ 158.1,
10
11 147.2, 147.0, 145.8, 133.7, 133.6, 130.1, 129.7, 128.0, 124.1, 123.5, 123.3, 122.3,
12
13 122.2, 120.3, 118.2, 111.8, 67.0, 66.7, 57.8, 53.4, 47.3, 40.9. HPLC purity: 99.7%.
14
15 HRMS (ESI) m/z : calcd for C₂₄H₂₄N₆O₂, [M+H]⁺ 429.2034, found 429.2021.
16
17

18
19 *N*-((1-(2-(pyrrolidin-1-yl)ethyl)-1H-1,2,3-triazol-4-yl)methyl)benzofuro[3,2-*b*)
20
21 *quinolin-11-amine* (**5e**). Compound **2** was treated with **3e** according to general
22
23 procedure to afford **5e** as a white solid. Yield 79%. m.p. 198.7-199.0 °C; ¹H NMR
24
25 (400 MHz, CDCl₃) δ 8.37 (d, $J = 7.7$ Hz, 1H), 8.18 (d, $J = 8.5$ Hz, 1H), 7.92 (d, $J =$
26
27 8.4 Hz, 1H), 7.67 (d, $J = 11.3$ Hz, 2H), 7.60 (t, $J = 7.3$ Hz, 2H), 7.45 (dd, $J = 13.9, 6.8$
28
29 Hz, 2H), 5.71 (t, $J = 5.4$ Hz, 1H), 5.36 (d, $J = 6.1$ Hz, 2H), 4.41 (t, $J = 6.3$ Hz, 2H),
30
31 2.87 (t, $J = 6.3$ Hz, 2H), 2.43 (s, 4H), 1.64 (s, 4H). ¹³C NMR (101 MHz, CDCl₃) δ
32
33 158.1, 147.1, 146.9, 145.6, 133.7, 133.6, 130.0, 129.6, 128.0, 124.1, 123.5, 123.2,
34
35 122.4, 122.2, 120.3, 118.1, 111.7, 55.3, 53.9, 49.4, 40.98, 23.5. HPLC purity : 99.4%.
36
37
38
39 HRMS (ESI) m/z : calcd for C₂₄H₂₄N₆O, [M+H]⁺ 413.2084, found 413.2070.
40
41

42
43 *N*-((1-(2-(piperidin-1-yl)ethyl)-1H-1,2,3-triazol-4-yl)methyl)benzofuro[3,2-*b*)
44
45 *quinolin-11-amine* (**5f**). Compound **2** was treated with **3f** according to general
46
47 procedure to afford **5f** as a white solid. 88% yield. m.p. 222.5-223.1 °C; ¹H NMR (400
48
49 MHz, CDCl₃) δ 8.37 (d, $J = 7.7$ Hz, 1H), 8.18 (d, $J = 8.4$ Hz, 1H), 7.92 (d, $J = 8.3$ Hz,
50
51 1H), 7.65 (dd, $J = 4.4, 3.0$ Hz, 2H), 7.64-7.56 (m, 3H), 7.47-7.41 (m, 2H), 5.76 (s,
52
53 1H), 5.36 (d, $J = 6.2$ Hz, 2H), 4.37 (t, $J = 6.2$ Hz, 2H), 2.66 (t, $J = 6.2$ Hz, 2H), 2.29 (s,
54
55 4H), 1.32 (s, 6H). ¹³C NMR (101 MHz, CDCl₃) δ 158.1, 147.1, 146.9, 145.5, 133.7,
56
57 130.0, 129.6, 128.0, 124.1, 123.4, 123.2, 122.5, 122.2, 120.3, 118.1, 111.8, 58.0, 54.4,
58
59
60

1
2
3 47.7, 41.0, 25.8, 24.1. HPLC purity : 100.0%. HRMS (ESI) m/z : calcd for $C_{25}H_{26}N_6O$,
4
5
6 $[M+H]^+$ 427.2241, found 427.2221.

7
8 *N-((1-(2-(4-methylpiperazin-1-yl)ethyl)-1H-1,2,3-triazol-4-yl)methyl)benzofuro*
9
10 *[3,2-b]quinolin-11-amine (5g)*. Compound **2** was treated with **3g** according to general
11 procedure to afford **5g** as a pale yellow solid. 82% yield. m.p. 214.8-215.7 °C; 1H
12 NMR (400 MHz, $CDCl_3$) δ 8.37 (d, $J = 8.5$ Hz, 1H), 8.18 (d, $J = 9.3$ Hz, 1H), 7.92 (d,
13 $J = 8.0$ Hz, 1H), 7.68-7.64 (m, 1H), 7.63 (s, 1H), 7.61 (dt, $J = 7.5, 3.6$ Hz, 2H),
14 7.49-7.42 (m, 2H), 5.73 (t, $J = 6.1$ Hz, 1H), 5.36 (d, $J = 6.3$ Hz, 2H), 4.37 (t, $J = 6.1$
15 Hz, 2H), 2.71 (t, $J = 6.1$ Hz, 2H), 2.39 (s, 4H), 2.17 (s, 8H). ^{13}C NMR (101 MHz,
16 $CDCl_3$) δ 158.1, 147.2, 147.0, 145.7, 133.7, 133.6, 130.1, 129.7, 128.0, 124.1, 123.5,
17 123.3, 122.4, 122.2, 120.3, 118.2, 111.8, 57.2, 54.8, 52.9, 47.5, 45.8, 41.0. HPLC
18 purity: 98.8%. HRMS (ESI) m/z : calcd for $C_{25}H_{27}N_7O$, $[M+H]^+$ 442.2350, found
19 442.2344.

20
21
22 *N-((1-(3-(dimethylamino)propyl)-1H-1,2,3-triazol-4-yl)methyl)benzofuro[3,2-b]*
23 *quinolin-11-amine (5h)*. Compound **2** was treated with **3h** according to general
24 procedure to afford **5h** as a white solid. 89% yield. m.p. 188.0-188.9 °C; 1H NMR
25 (400 MHz, $CDCl_3$) δ 8.38 (d, $J = 7.6$ Hz, 1H), 8.19 (d, $J = 8.5$ Hz, 1H), 7.94 (d, $J =$
26 8.5 Hz, 1H), 7.69-7.58 (m, 3H), 7.54 (s, 1H), 7.46 (td, $J = 8.0, 1.5$ Hz, 2H), 5.75 (s,
27 1H), 5.37 (d, $J = 6.1$ Hz, 2H), 4.39 (t, $J = 6.8$ Hz, 2H), 2.24 (t, $J = 6.8$ Hz, 2H), 2.16 (s,
28 6H), 2.07-2.02 (m, 2H). ^{13}C NMR (101 MHz, $CDCl_3$) δ 158.1, 147.2, 147.0, 145.6,
29 133.7, 133.6, 130.0, 129.7, 128.0, 124.1, 123.5, 123.2, 122.1, 122.1, 120.3, 118.1,
30 111.8, 55.7, 48.05, 45.2, 41.0, 28.1. HPLC purity: 99.7%. HRMS (ESI) m/z : calcd for
31 $C_{23}H_{24}N_6O$, $[M+H]^+$ 401.2084, found 401.2089.

32
33 *N-((1-(3-(diethylamino)propyl)-1H-1,2,3-triazol-4-yl)methyl)benzofuro[3,2-b]qu*
34 *inolin-11-amine (5i)*. Compound **2** was treated with **3i** according to general procedure
35
36
37
38
39
40
41
42
43
44
45
46
47
48
49
50
51
52
53
54
55
56
57
58
59
60

1
2
3 to afford **5i** as a white solid. 89% yield. m.p. 150.2-151.1 °C; ¹H NMR (400 MHz,
4 CDCl₃) δ 8.36 (d, *J* = 7.5 Hz, 1H), 8.18 (d, *J* = 9.3 Hz, 1H), 7.93 (d, *J* = 8.0 Hz, 1H),
5 7.68-7.57 (m, 3H), 7.49 (s, 1H), 7.45 (dtd, *J* = 8.0, 6.2, 1.5 Hz, 2H), 5.73 (t, *J* = 6.1
6 Hz, 1H), 5.36 (d, *J* = 6.2 Hz, 2H), 4.35 (t, *J* = 7.0 Hz, 2H), 2.41 (q, *J* = 7.1 Hz, 4H),
7 2.34 (t, *J* = 6.8 Hz, 2H), 1.99 (p, *J* = 6.9 Hz, 2H), 0.89 (t, *J* = 7.1 Hz, 6H). ¹³C NMR
8 (101 MHz, CDCl₃) δ 158.1, 147.3, 147.0, 145.7, 133.7, 133.6, 130.0, 129.7, 128.0,
9 124.1, 123.5, 123.2, 122.1, 122.0, 120.3, 118.2, 111.8, 49.2, 48.4, 46.5, 41.0, 27.9,
10 11.4. HPLC purity: 99.9%. HRMS (ESI) *m/z*: calcd for C₂₅H₂₈N₆O, [M+H]⁺ 429.2397,
11 found 429.2401.
12
13

14
15
16
17
18
19
20
21
22
23 *N*-((1-(3-aminopropyl)-1*H*-1,2,3-triazol-4-yl)methyl)benzofuro[3,2-*b*]quinolin-11
24 -amine (**5j**). Compound **2** was treated with **3j** according to general procedure to afford
25 **5j** as a yellow solid. 72% yield. m.p. 129.8-130.5 °C; ¹H NMR (400 MHz, CDCl₃) δ
26 8.37 (d, *J* = 7.6 Hz, 1H), 8.18 (d, *J* = 7.8 Hz, 1H), 7.93 (d, *J* = 8.4 Hz, 1H), 7.69-7.64
27 (m, 1H), 7.61 (dt, *J* = 8.8, 4.3 Hz, 2H), 7.51-7.49 (m, 1H), 7.48-7.42 (m, 2H), 5.69 (s,
28 1H), 5.36 (d, *J* = 6.2 Hz, 2H), 4.41 (t, *J* = 6.9 Hz, 2H), 2.63 (t, *J* = 6.6 Hz, 2H), 1.95
29 (p, *J* = 6.8 Hz, 2H). ¹³C NMR (101 MHz, MeOD) δ 157.9, 146.9, 146.2, 146.2, 135.4,
30 132.9, 130.1, 128.2, 127.4, 123.6, 123.0, 122.5, 122.3, 121.5, 121.3, 118.0, 111.7,
31 47.4, 40.00, 37.7, 32.4. HPLC purity: 98.8%. HRMS (ESI) *m/z*: calcd for C₂₁H₂₀N₆O,
32 [M+H]⁺ 373.1771, found 373.1756.
33
34
35
36
37
38
39
40
41
42
43
44

45
46
47 *N*-((1-(3-morpholinopropyl)-1*H*-1,2,3-triazol-4-yl)methyl)benzofuro[3,2-*b*]
48 quinolin-11-amine (**5k**). Compound **2** was treated with **3k** according to general
49 procedure to afford **5k** as a white solid. 88% yield. m.p. 192.6-193.5 °C; ¹H NMR
50 (400 MHz, CDCl₃) δ 8.47 (d, *J* = 8.2 Hz, 1H), 8.19 (d, *J* = 8.5 Hz, 1H), 7.95 (d, *J* =
51 8.6 Hz, 1H), 7.61 (dt, *J* = 12.6, 8.0 Hz, 4H), 7.43 (dt, *J* = 25.4, 7.5 Hz, 2H), 5.40 (d, *J*
52 = 5.9 Hz, 2H), 4.40 (t, *J* = 6.8 Hz, 2H), 3.64-3.55 (m, 4H), 2.25 (dd, *J* = 17.5, 10.9 Hz,
53 54 55 56 57 58 59 60

1
2
3 6H), 2.03 (dt, $J = 13.4, 6.5$ Hz, 2H). ^{13}C NMR (101 MHz, CDCl_3) δ 158.1, 147.1,
4
5 146.9, 145.7, 133.6, 133.6, 130.1, 129.6, 128.1, 124.2, 123.4, 123.3, 122.2, 122.0,
6
7 120.2, 118.1, 111.7, 66.8, 54.7, 53.4, 48.0, 41.0, 26.9. HPLC purity: 99.9%. HRMS
8
9 (ESI) m/z : calcd for $\text{C}_{25}\text{H}_{26}\text{N}_6\text{O}_2$, $[\text{M}+\text{H}]^+$ 443.2190, found 443.2196.

10
11 *N*-((1-(3-(pyrrolidin-1-yl)propyl)-1*H*-1,2,3-triazol-4-yl)methyl)benzofuro[3,2-*b*]
12
13 *quinolin-11-amine* (**5l**). Compound **2** was treated with **3l** according to general
14
15 procedure to afford **5l** as a white solid. 84% yield. m.p. 194.7-195.3 °C; ^1H NMR (400
16
17 MHz, CDCl_3) δ 8.36 (d, $J = 7.6$ Hz, 1H), 8.17 (dd, $J = 8.5, 0.7$ Hz, 1H), 7.93 (d, $J =$
18
19 8.2 Hz, 1H), 7.68-7.62 (m, 1H), 7.62-7.56 (m, 2H), 7.49 (s, 1H), 7.47-7.41 (m, 2H),
20
21 5.77 (t, $J = 6.1$ Hz, 1H), 5.35 (d, $J = 6.2$ Hz, 2H), 4.37 (t, $J = 6.9$ Hz, 2H), 2.40-2.30
22
23 (m, 6H), 2.01 (p, $J = 6.9$ Hz, 2H), 1.74-1.61 (m, 4H). ^{13}C NMR (101 MHz, CDCl_3) δ
24
25 158.1, 147.2, 147.0, 145.7, 133.7, 133.6, 130.0, 129.6, 128.0, 124.0, 123.5, 123.2,
26
27 122.1, 122.1, 120.3, 118.2, 111.8, 53.9, 52.4, 48.3, 40.9, 29.3, 23.4. HPLC purity:
28
29 99.8%. HRMS (ESI) m/z : calcd for $\text{C}_{25}\text{H}_{26}\text{N}_6\text{O}$, $[\text{M}+\text{H}]^+$ 427.2241, found 427.2243.

30
31
32
33
34 *N*-((1-(3-(piperidin-1-yl)propyl)-1*H*-1,2,3-triazol-4-yl)methyl)benzofuro[3,2-*b*]
35
36 *quinolin-11-amine* (**5m**). Compound **2** was treated with **3m** according to general
37
38 procedure to afford **5m** as a white solid. 86% yield. m.p. 193.9-194.7 °C; ^1H NMR
39
40 (400 MHz, CDCl_3) δ 8.37 (d, $J = 7.6$ Hz, 1H), 8.18 (d, $J = 8.5$ Hz, 1H), 7.92 (d, $J =$
41
42 8.5 Hz, 1H), 7.63 (dt, $J = 17.0, 8.1$ Hz, 3H), 7.51 – 7.41 (m, 3H), 5.72 (s, 1H), 5.36 (d,
43
44 $J = 5.4$ Hz, 2H), 4.35 (t, $J = 6.4$ Hz, 2H), 2.31 (s, 6H), 2.22 (s, 6H), 1.99 (dt, $J = 12.6,$
45
46 6.2 Hz, 2H). ^{13}C NMR (101 MHz, CDCl_3) δ 158.1, 147.2, 146.9, 145.7, 133.7, 133.6,
47
48 130.1, 129.6, 128.1, 124.1, 123.4, 123.3, 122.2, 122.1, 120.3, 118.1, 111.8, 55.1, 54.4,
49
50 48.3, 41.0, 27.3, 25.8, 24.3. HPLC purity: 99.8%. HRMS (ESI) m/z : calcd for
51
52 $\text{C}_{26}\text{H}_{28}\text{N}_6\text{O}$, $[\text{M}+\text{H}]^+$ 441.2397, found 441.2396.

53
54
55
56
57
58
59
60
N-((1-(3-(4-methylpiperazin-1-yl)propyl)-1*H*-1,2,3-triazol-4-yl)methyl)

1
2
3 *benzofuro[3,2-b]quinolin-11-amine (5n)*. Compound **2** was treated with **3n** according
4
5 to general procedure to afford **5n** as a white solid. 70% yield. m.p.158.0-161.1 °C; ¹H
6
7 NMR (400 MHz, CDCl₃) δ 8.37 (d, *J* = 7.6 Hz, 1H), 8.18 (d, *J* = 8.5 Hz, 1H), 7.92 (d,
8
9 *J* = 8.5 Hz, 1H), 7.63 (dt, *J* = 17.0, 8.1 Hz, 3H), 7.46 (s, 3H), 5.72 (s, 1H), 5.36 (d, *J* =
10
11 5.4 Hz, 2H), 4.35 (t, *J* = 6.4 Hz, 2H), 2.31 (s, 6H), 2.21 (d, *J* = 12.2 Hz, 6H),
12
13 2.07-1.91 (m, 3H). ¹³C NMR (101 MHz, CDCl₃) δ 158.1, 147.1, 146.9, 145.7, 133.6,
14
15 133.6, 130.1, 129.6, 128.0, 124.1, 123.4, 123.3, 122.2, 122.1, 120.3, 118.1, 111.8,
16
17 54.9, 54.1, 52.8, 48.0, 45.9, 40.9, 27.2. HPLC purity: 99.5%. HRMS (ESI) *m/z*: calcd
18
19 for C₂₆H₂₉N₇O, [M+H]⁺ 456.2506, found 456.2516.
20
21

22
23 *2-(4-((benzofuro[3,2-b]quinolin-11-ylamino)methyl)-1H-1,2,3-triazol-1-yl)ethan*
24
25 *-1-ol (6a)*. Compound **2** was treated with **4a** according to general procedure to afford
26
27 **6a** as a white solid. 76% yield. m.p.180.9-181.8 °C; ¹H NMR (400 MHz, DMSO) δ
28
29 8.47 (d, *J* = 8.3 Hz, 1H), 8.27 (d, *J* = 7.6 Hz, 1H), 8.03 (d, *J* = 8.3 Hz, 1H), 7.99 (s,
30
31 1H), 7.81 (d, *J* = 8.5 Hz, 1H), 7.73 (d, *J* = 5.8 Hz, 2H), 7.52 (dd, *J* = 14.5, 7.4 Hz, 2H),
32
33 5.25 (d, *J* = 6.2 Hz, 2H), 4.92 (t, *J* = 5.1 Hz, 1H), 4.31 (t, *J* = 5.3 Hz, 2H), 3.69 (dd, *J*
34
35 = 9.8, 4.6 Hz, 2H). ¹³C NMR (101 MHz, DMSO-*d*₆) δ 157.4, 146.7, 146.1, 145.9,
36
37 134.7, 132.7, 130.1, 128.9, 127.9, 123.3, 123.2, 123.1, 123.0, 122.3, 121.4, 118.1,
38
39 112.3, 59.8, 52.0, 40.0. HPLC purity: 99.3%. HRMS (ESI) *m/z*: calcd for,
40
41 [M+H]⁺, 360.1455, found 360.1449.
42
43

44
45 *3-(4-((benzofuro[3,2-b]quinolin-11-ylamino)methyl)-1H-1,2,3-triazol-1-yl)*
46
47 *propan-1-ol (6b)*. Compound **2** was treated with **4b** according to general procedure to
48
49 afford **6b** as a gray solid. Yield 75. m.p.191.2-192.6 °C; ¹H NMR (400 MHz, CDCl₃)
50
51 δ 8.37 (d, *J* = 7.7 Hz, 1H), 8.18 (d, *J* = 8.4 Hz, 1H), 7.92 (d, *J* = 8.4 Hz, 1H),
52
53 7.70-7.64 (m, 1H), 7.61 (dd, *J* = 11.4, 4.9 Hz, 2H), 7.51 (s, 1H), 7.46 (ddd, *J* = 9.4,
54
55 9.0, 4.9 Hz, 2H), 5.65 (s, 1H), 5.36 (d, *J* = 6.2 Hz, 2H), 4.46 (t, *J* = 6.7 Hz, 2H), 3.56
56
57
58
59
60

(t, $J = 4.7$ Hz, 2H), 2.11-2.03 (m, 2H). ^{13}C NMR (101 MHz, DMSO- d_6) δ 157.9, 147.1, 146.6, 146.5, 135.2, 133.1, 130.7, 129.3, 128.4, 123.8, 123.8, 123.4, 123.3, 122.9, 122.0, 118.6, 112.8, 57.9, 47.0, 40.5, 33.5. HPLC purity: 99.5%. HRMS (ESI) m/z : calcd for $\text{C}_{21}\text{H}_{19}\text{N}_5\text{O}_2$, $[\text{M}+\text{H}]^+$ 374.1612, found 374.1611.

N-((1-benzyl-1H-1,2,3-triazol-4-yl)methyl)benzofuro[3,2-b]quinolin-11-amine

(6c). Compound **2** was treated with **4c** according to general procedure to afford **6c** as a white solid. 55% yield. m.p. 190.9-191.9 °C; ^1H NMR (400 MHz, CDCl_3) δ 8.36 (d, $J = 7.6$ Hz, 1H), 8.18 (d, $J = 8.6$ Hz, 1H), 7.91 (d, $J = 8.6$ Hz, 1H), 7.66 (ddd, $J = 8.3$, 6.8, 1.2 Hz, 1H), 7.59 (ddd, $J = 8.4$, 7.2, 1.3 Hz, 1H), 7.52-7.43 (m, 3H), 7.41 (s, 1H), 7.30 (dd, $J = 5.0$, 1.9 Hz, 3H), 7.19 (dd, $J = 6.5$, 3.0 Hz, 2H), 5.63 (s, 1H), 5.47 (s, 2H), 5.33 (d, $J = 6.1$ Hz, 2H). ^{13}C NMR (101 MHz, CDCl_3) δ 158.1, 147.2, 146.9, 146.2, 134.4, 133.7, 133.5, 130.1, 129.6, 129.1, 129.1, 128.8, 128.0, 128.0, 127.9, 124.1, 123.4, 123.2, 122.2, 121.7, 120.2, 118.1, 111.8, 54.2, 41.0. HPLC purity: 99.9%. HRMS (ESI) m/z : calcd for $\text{C}_{25}\text{H}_{19}\text{N}_5\text{O}$, $[\text{M}+\text{H}]^+$ 406.1662, found 406.1647.

N-((1-phenethyl-1H-1,2,3-triazol-4-yl)methyl)benzofuro[3,2-b]quinolin-11-amine

e (6d). Compound **2** was treated with **4d** according to general procedure to afford **6d** as a white solid. 60% yield. m.p. 172.5-173.8 °C; ^1H NMR (400 MHz, DMSO- d_6) δ 8.41 (d, $J = 8.4$ Hz, 1H), 8.22 (d, $J = 7.5$ Hz, 1H), 8.02 (d, $J = 8.3$ Hz, 1H), 7.85 (d, $J = 16.0$ Hz, 2H), 7.70 (dt, $J = 11.2$, 7.7 Hz, 3H), 7.47 (t, $J = 6.9$ Hz, 2H), 7.02-6.94 (m, 4H), 5.16 (d, $J = 5.8$ Hz, 2H), 4.49 (t, $J = 7.0$ Hz, 2H), 3.01 (t, $J = 7.0$ Hz, 2H). ^{13}C NMR (101 MHz, DMSO- d_6) δ 157.9, 146.6, 138.0, 135.1, 133., 130.7, 129.4, 128.9, 128.6, 128.4, 126.8, 123.8, 123.5, 123.0, 122.8, 122.0, 118.6, 112.8, 50.8, 40.6, 40.4, 40.2, 40.0, 39.8, 39.6, 39.4, 36.2. HPLC purity: 99.8%. HRMS (ESI) m/z : calcd for $\text{C}_{26}\text{H}_{21}\text{N}_5\text{O}$, $[\text{M}+\text{H}]^+$ 420.1819, found 420.1818.

N-((1-(3-phenylpropyl)-1H-1,2,3-triazol-4-yl)methyl)benzofuro[3,2-b]quinolin-11-amine

1
2
3 *l*-amine (**6e**). Compound **2** was treated with **4e** according to general procedure to
4 afford **6e** as a white solid. 58% yield. m.p.160.3-161.2 °C; ¹H NMR (400 MHz,
5 CDCl₃) δ 8.38 (d, *J* = 7.6 Hz, 1H), 8.17 (d, *J* = 8.4 Hz, 1H), 7.94 (d, *J* = 8.4 Hz, 1H),
6
7 7.68-7.54 (m, 3H), 7.48-7.39 (m, 3H), 7.25-7.13 (m, 3H), 7.06 (d, *J* = 7.0 Hz, 2H),
8
9 5.87 (s, 1H), 5.35 (d, *J* = 5.8 Hz, 2H), 4.27 (t, *J* = 7.1 Hz, 2H), 2.57 (t, *J* = 7.5 Hz, 2H),
10
11 2.21-2.15 (m, 2H). ¹³C NMR (101 MHz, CDCl₃) δ 158.1, 147.2, 146.9, 145.8, 139.9,
12
13 133.7, 133.6, 130.1, 129.6, 128.6, 128.3, 128.0, 126.3, 124.1, 123.5, 123.2, 122.,
14
15 121.6, 120.3, 118.1, 111.8, 49.5, 41.0, 32.4, 31.5. HPLC purity: 99.9%. HRMS (ESI)
16
17 *m/z*: calcd for C₂₇H₂₃N₅O, [M+H]⁺ 434.1975, found 434.1976.
18
19
20
21
22

23 *N*-((1-propyl-1*H*-1,2,3-triazol-4-yl)methyl)benzofuro[3,2-*b*]quinolin-11-amine

24
25 (**6f**). Compound **2** was treated with **4f** according to general procedure to afford **6f** as a
26 yellow solid. 58% yield. m.p.178.9-181.2 °C; ¹H NMR (400 MHz, CDCl₃) δ 8.35 (d,
27
28 *J* = 7.8 Hz, 1H), 8.14 (d, *J* = 8.5 Hz, 1H), 7.94 (d, *J* = 8.3 Hz, 1H), 7.64-7.52 (m, 3H),
29
30 7.50 (s, 1H), 7.44-7.35 (m, 2H), 5.98 (d, *J* = 5.8 Hz, 1H), 5.31 (d, *J* = 5.8 Hz, 2H),
31
32 4.41-4.29 (m, 1H), 2.12 (d, *J* = 12.7 Hz, 2H), 1.85 (d, *J* = 13.5 Hz, 2H), 1.67 (dd, *J* =
33
34 26.5, 14.1 Hz, 3H), 1.39 (dd, *J* = 26.0, 12.9 Hz, 2H), 1.21 (dd, *J* = 24.6, 11.9 Hz, 1H).
35
36 ¹³C NMR (101 MHz, CDCl₃) δ 158.0, 147.0, 146.8, 145.9, 133.9, 133.6, 130.0, 129.4,
37
38 128.0, 124.0, 123.4, 123.2, 122.1, 121.7, 120.6, 118.1, 111.8, 51.9, 40.9, 23.6, 11.0.
39
40 HPLC purity: 98.3%. HRMS (ESI) *m/z*: calcd for C₂₁H₁₉N₅O, [M+H]⁺ 358.1662,
41
42 found 358.1657.
43
44
45
46

47 *N*-((1-isopentyl-1*H*-1,2,3-triazol-4-yl)methyl)benzofuro[3,2-*b*]quinolin-11-amine

48
49 (**6g**). Compound **2** was treated with **4g** according to general procedure to afford **6g** as
50 a white solid. 62% yield. m.p. 149.1-152.0 °C; ¹H NMR (400 MHz, CDCl₃) δ 8.38 (d,
51
52 *J* = 7.7 Hz, 1H), 8.18 (d, *J* = 9.3 Hz, 1H), 7.93 (d, *J* = 8.0 Hz, 1H), 7.68-7.56 (m, 3H),
53
54 7.48 (s, 1H), 7.47-7.41 (m, 2H), 5.82 (s, 1H), 5.35 (d, *J* = 5.9 Hz, 2H), 4.33-4.28 (m,
55
56
57
58
59
60

2H), 1.73 (dd, $J = 14.9, 7.1$ Hz, 2H), 1.55-1.44 (m, 1H), 0.89 (d, $J = 6.6$ Hz, 6H). ^{13}C NMR (101 MHz, CDCl_3) δ 158.1, 147.0, 146.8, 145.8, 133.7, 133.6, 130.1, 129.4, 128.1, 124.1, 123.3, 123.2, 122.2, 121.5, 120.4, 118.1, 111.8, 48.7, 40.9, 38.9, 25.4, 22.1. HPLC purity: 96.9%. HRMS (ESI) m/z : calcd for $\text{C}_{23}\text{H}_{23}\text{N}_5\text{O}$, $[\text{M}+\text{H}]^+$ 386.1975, found 386.1969.

N-((1-cyclopentyl-1H-1,2,3-triazol-4-yl)methyl)benzofuro[3,2-b]quinolin-11-amine (6h). Compound **2** was treated with **4h** according to general procedure to afford **6h** as a pale yellow solid. 56% yield. m.p. 156.6-157.9 °C; ^1H NMR (400 MHz, CDCl_3) δ 8.38 (t, $J = 8.6$ Hz, 1H), 8.17 (t, $J = 8.0$ Hz, 1H), 7.94 (d, $J = 8.5$ Hz, 1H), 7.68-7.55 (m, 3H), 7.53 (d, $J = 7.7$ Hz, 1H), 7.42 (dt, $J = 14.5, 7.2$ Hz, 2H), 5.92 (s, 1H), 5.38-5.27 (m, 2H), 4.92-4.81 (m, 1H), 2.27-2.14 (m, 2H), 2.05-1.93 (m, 2H), 1.85 (tt, $J = 11.1, 5.8$ Hz, 2H), 1.72 (dt, $J = 11.1, 4.7$ Hz, 2H). ^{13}C NMR (101 MHz, CDCl_3) δ 158.0, 147.0, 146.7, 145.4, 133.9, 133.6, 130.1, 129.3, 128.1, 124.0, 123.3, 123.2, 122.2, 120.4, 120.4, 118.0, 111.7, 61.9, 40.9, 33.3, 24.0. HPLC purity: 96.3%. HRMS (ESI) m/z : calcd for $\text{C}_{23}\text{H}_{21}\text{N}_5\text{O}$, $[\text{M}+\text{H}]^+$ 384.1819, found 384.1815.

N-((1-cyclohexyl-1H-1,2,3-triazol-4-yl)methyl)benzofuro[3,2-b]quinolin-11-amine (6i). Compound **2** was treated with **4i** according to general procedure to afford **6i** as a white solid. 62% yield. m.p. 156.6-157.9 °C; ^1H NMR (400 MHz, CDCl_3) δ 8.38 (t, $J = 8.6$ Hz, 1H), 8.17 (t, $J = 8.0$ Hz, 1H), 7.94 (d, $J = 8.5$ Hz, 1H), 7.68-7.55 (m, 3H), 7.53 (d, $J = 7.7$ Hz, 1H), 7.42 (dt, $J = 14.5, 7.2$ Hz, 2H), 5.92 (s, 1H), 5.38-5.27 (m, 2H), 4.92-4.81 (m, 1H), 2.27-2.14 (m, 2H), 2.05-1.93 (m, 2H), 1.85 (tt, $J = 11.1, 5.8$ Hz, 2H), 1.72 (dt, $J = 11.1, 4.7$ Hz, 2H). ^{13}C NMR (101 MHz, CDCl_3) δ 158.1, 147.1, 146.9, 145.2, 133.8, 133.6, 130.1, 129.4, 128.0, 124.0, 123.4, 123.2, 122.2, 120.4, 119.6, 118.1, 111.8, 60.2, 41.0, 33.5, 25.1, 25.0. HPLC purity: 98.7%. HRMS (ESI) m/z : calcd for $\text{C}_{24}\text{H}_{23}\text{N}_5\text{O}$, $[\text{M}+\text{H}]^+$ 398.1975, found 398.1976.

1
2
3
4
5
6
7
8
9
10
11
12
13
14
15
16
17
18
19
20
21
22
23
24
25
26
27
28
29
30
31
32
33
34
35
36
37
38
39
40
41
42
43
44
45
46
47
48
49
50
51
52
53
54
55
56
57
58
59
60

(2*S*,3*S*,4*R*,5*S*,6*S*)-2-(acetoxymethyl)-6-(4-((benzofuro[3,2-*b*]quinolin-11-ylamino)methyl)-1*H*-1,2,3-triazol-1-yl)tetrahydro-2*H*-pyran-3,4,5-triyl triacetate (**6j**).

Compound **2** was treated with **4j** according to general procedure to afford **6j** as a white solid. Yield 78%. m.p. 210.7-211.1 °C; ¹H NMR (400 MHz, CDCl₃) δ 8.38 (d, *J* = 7.7 Hz, 1H), 8.19 (dd, *J* = 8.5, 0.7 Hz, 1H), 7.93 (d, *J* = 8.3 Hz, 1H), 7.78 (s, 1H), 7.65 (ddd, *J* = 4.9, 4.2, 1.1 Hz, 1H), 7.63-7.58 (m, 2H), 7.45 (ddd, *J* = 7.9, 7.2, 1.5 Hz, 2H), 5.85-5.80 (m, 1H), 5.71 (s, 1H), 5.43-5.31 (m, 4H), 5.19 (ddd, *J* = 9.5, 5.4, 3.9 Hz, 1H), 4.25 (dd, *J* = 12.6, 4.9 Hz, 1H), 4.10 (dd, *J* = 12.6, 2.0 Hz, 1H), 3.97 (ddd, *J* = 10.1, 4.9, 2.1 Hz, 1H), 2.05 (s, 3H), 2.01 (s, 3H), 2.00 (s, 3H), 1.67 (s, 3H). ¹³C NMR (101 MHz, CDCl₃) δ 170.5, 169.9, 169.4, 168.8, 158.2, 147.0, 146.6, 146.6, 133.7, 133.6, 130.2, 129.3, 128.1, 124.1, 123.3, 123.2, 122.2, 120.4, 120.2, 118.0, 111.9, 85.7, 75.1, 72.5, 70.1, 67.6, 61.5, 40.9, 20.6, 20.5, 20.5, 19.9. HPLC purity: 99.7%. HRMS (ESI) *m/z*: calcd for C₃₂H₃₁N₅O₁₀, [M+H]⁺ 646.2144, found 646.2152.

(2*S*,3*S*,4*S*,5*R*)-2-(acetoxymethyl)-5-(4-((benzofuro[3,2-*b*]quinolin-11-ylamino)methyl)-1*H*-1,2,3-triazol-1-yl)tetrahydrofuran-3,4-diyl diacetate (**6k**). Compound **2** was treated with **4k** according to general procedure to afford **6k** as a white solid. 68% yield. m.p. 159.5-160.3 °C; ¹H NMR (400 MHz, CDCl₃) δ 8.40 (d, *J* = 7.7 Hz, 1H), 8.18 (d, *J* = 7.8 Hz, 1H), 7.94 (d, *J* = 8.0 Hz, 1H), 7.76 (s, 1H), 7.61 (tt, *J* = 12.5, 7.1 Hz, 3H), 7.48-7.41 (m, 2H), 6.09 (d, *J* = 3.8 Hz, 1H), 5.84 (dd, *J* = 5.2, 3.8 Hz, 1H), 5.59 (t, *J* = 5.3 Hz, 1H), 5.40 (t, *J* = 5.3 Hz, 2H), 4.44 (td, *J* = 4.9, 3.2 Hz, 1H), 4.35 (dd, *J* = 12.3, 3.1 Hz, 1H), 4.19 (dd, *J* = 12.3, 4.7 Hz, 1H), 2.11 (s, 3H), 2.08 (s, 3H), 1.96 (s, 3H). ¹³C NMR (101 MHz, CDCl₃) δ 170.3, 169.4, 169.2, 158.1, 146.7, 146.6, 146.2, 133.7, 130.2, 129.4, 128.2, 124.2, 123.3, 123.2, 122.3, 121.4, 120.3, 118.0, 111.9, 90.0, 81.0, 74.2, 70.8, 62.9, 40.9, 20.5, 20.5, 20.4. HPLC purity: 99.1%. HRMS (ESI) *m/z*: calcd for C₂₉H₂₇N₅O₈, [M+H]⁺ 574.1932, found 574.1948.

1
2
3
4
5
6
7
8
9
10
11
12
13
14
15
16
17
18
19
20
21
22
23
24
25
26
27
28
29
30
31
32
33
34
35
36
37
38
39
40
41
42
43
44
45
46
47
48
49
50
51
52
53
54
55
56
57
58
59
60

(2*S*,3*S*,4*R*,5*R*,6*S*)-2-(4-((benzofuro[3,2-*b*]quinolin-11-ylamino)methyl)-1*H*-1,2,3-triazol-1-yl)-6-(hydroxymethyl)tetrahydro-2*H*-pyran-3,4,5-triol (**6l**). A solution of 1M NaOH (10 mL) was added, at room temperature, to a solution of **6j** (0.645 g 1mmol) in 20 mL of MeOH. The mixture was stirred at room temperature and was monitored intermittently by TLC. Methanol was removed in vacuum and the white precipitate was filtered and washed with water and MeOH for few times to afford **6l** as a white solid. 88% yield. m.p. 214.7-215.6 °C; ¹H NMR (400 MHz, DMSO-*d*₆) δ 8.42 (d, *J* = 8.5 Hz, 1H), 8.22 (d, *J* = 7.6 Hz, 1H), 8.17 (s, 1H), 8.01 (d, *J* = 8.4 Hz, 1H), 7.78 (d, *J* = 8.3 Hz, 1H), 7.68 (t, *J* = 7.8 Hz, 2H), 7.47 (t, *J* = 7.4 Hz, 2H), 5.46 (d, *J* = 9.3 Hz, 1H), 5.26 (t, *J* = 5.4 Hz, 3H), 5.19 (d, *J* = 4.9 Hz, 1H), 5.09 (d, *J* = 5.5 Hz, 1H), 4.52 (t, *J* = 5.4 Hz, 1H), 3.73 (td, *J* = 9.1, 6.1 Hz, 1H), 3.62 (dd, *J* = 10.0, 5.5 Hz, 1H), 3.16 (td, *J* = 9.0, 5.7 Hz, 1H). ¹³C NMR (101 MHz, DMSO-*d*₆) δ 157.4, 145.9, 135.0, 132.6, 130.3, 128.5, 128.1, 123.4, 123.3, 122.7, 122.4, 122.2, 121.5, 118.0, 112.4, 87.3, 79.9, 77.0, 71.9, 69.5, 60.7. HPLC purity: 99.5%. HRMS (ESI) *m/z*: calcd for C₂₄H₂₃N₅O₆, [M+H]⁺ 478.1721, found 478.1725.

(2*R*,3*S*,4*R*,5*R*)-2-(4-((benzofuro[3,2-*b*]quinolin-11-ylamino)methyl)-1*H*-1,2,3-triazol-1-yl)-5-(hydroxymethyl)tetrahydrofuran-3,4-diol (**6m**) Compound **6k** (0.573 g 1mmol) was treated according to the procedure for the de-protection of **6l** to afford **6m** as a white solid. 92% yield. ¹H NMR (400 MHz, DMSO-*d*₆) δ 8.42 (d, *J* = 8.5 Hz, 1H), 8.30 (s, 1H), 8.21 (d, *J* = 7.5 Hz, 1H), 8.01 (d, *J* = 8.1 Hz, 1H), 7.84 (t, *J* = 6.3 Hz, 1H), 7.78 (d, *J* = 8.3 Hz, 1H), 7.66 (td, *J* = 7.4, 3.2 Hz, 2H), 7.47 (td, *J* = 7.4, 2.6 Hz, 2H), 5.88 (d, *J* = 4.7 Hz, 1H), 5.49 (d, *J* = 6.1 Hz, 1H), 5.20 (dd, *J* = 10.2, 5.9 Hz, 3H), 4.90 (t, *J* = 5.3 Hz, 1H), 4.32 (dd, *J* = 10.5, 5.0 Hz, 1H), 4.07 (dd, *J* = 9.5, 4.8 Hz, 1H), 3.91 (q, *J* = 4.2 Hz, 1H), 3.53 (dt, *J* = 11.4, 4.7 Hz, 1H), 3.47-3.39 (m, 1H). ¹³C NMR (101 MHz, DMSO-*d*₆) δ 172.8, 157.9, 147.2, 135.2, 133.1, 130.7, 129.4, 128.4,

1
2
3 123.8, 123.5, 122.9, 122.2, 122.0, 118.6, 112.8, 92.4, 86.3, 75.5, 70.9, 61.9, 40.4.
4
5 HPLC purity: 99.4%. HRMS (ESI) m/z : calcd for $C_{23}H_{21}N_5O_5$, $[M+H]^+$ 448.1615,
6
7 found 448.1613.
8
9

10
11 **Fluorescence resonance energy transfer (FRET).** FRET assay was
12 carried out on a real-time PCR apparatus following previously published
13 procedures.^{17, 22, 34} The oligomers labeled with FAM (donor fluorophore, FAM:
14 6-carboxyfluorescein) and TAMRA (acceptor fluorophore, TAMRA:
15 6-carboxytetramethylrhodamine) were purchased from Invitrogen (China). The
16 fluorescently labeled oligonucleotides Fpu22T (Table S1) and F10T (Table S1) were
17 used. Fluorescence melting curves were determined with a Roche LightCycler 2
18 real-time PCR machine, using a total reaction volume of 20 μ L, with 0.4 μ M of
19 labeled oligonucleotide in Tris-HCl buffer (10 mM, pH 7.4) containing 10 mM KCl.
20 Measurements were made in triplicate with excitation at 470 nm and detection at 530
21 nm. Fluorescence readings were taken at an interval of 1 $^{\circ}$ C over the range 37-99 $^{\circ}$ C,
22 with a constant temperature being maintained for 30 s prior to each reading to ensure
23 a stable value. The melting of the G-quadruplex was monitored alone or in the
24 presence of compounds and/or double-stranded competitor ds26. Final analysis of the
25 data was carried out using Origin 9 (OriginLab Corp.).
26
27
28
29
30
31
32
33
34
35
36
37
38
39
40
41
42
43
44
45

46
47 **Surface Plasmon Resonance (SPR).** SPR measurements were performed
48 on a ProteOn XPR36 Protein Interaction Array system (Bio-Rad Laboratories,
49 Hercules, CA) using a neutravidin-coated NLC sensor chip. In a typical experiment,
50 biotinylated duplex DNA and biotinylated Pu22 were folded in filtered and degassed
51 running buffer (Tris-HCl 50 mM pH7.4, 100 mM KCl). The DNA samples were then
52
53
54
55
56
57
58
59
60

1
2
3 captured (1,000 RU) in flow cells, and a blank cell was set as a control. Ligand
4 solutions (at 0.625, 1.25, 2.5, 5, 10 μM) were prepared within the running buffer by
5 serial dilutions from stock solutions. The NLC sensor chip was regenerated with a
6 short injection of 1 M KCl between consecutive measurements. The final graphs were
7 obtained by subtracting blank sensorgrams from the duplex or quadruplex
8 sensorgrams. The data were analyzed with ProteOn[®] manager software, using the
9 Langmuir model to fit the kinetic data.
10
11
12
13
14
15
16
17
18
19

20
21 **Competition dialysis assay.** The competition dialysis assay was conducted
22 according to the reference.³⁵ Briefly, 1 μM of compounds were placed into a 500 mL
23 volume beaker in a 10 mM Tris-HCl buffer (100 mM NaCl, pH 7.4). 250 μL
24 Slide-A-Lyzer dialysis cassettes (Thermo Scientific, USA) containing different
25 oligomers at 45 μM , including *c-myc* Pu27, *c-myc-mu*, hairpin DNA, bcl-2, H-Ras,
26 c-kit, RET, VEGF, HTG-21, and dT30, respectively, were placed in the beaker. The
27 contents of the beaker were allowed to equilibrate with continuous stirring for 24 h at
28 25 °C. At the end of the equilibration, DNA samples were carefully removed to
29 microfuge tubes and treated with 1% (w/v) sodium dodecyl sulfate (SDS) following
30 with a filtration using a 0.45 μm filter membrane. The total concentration of
31 compounds (C_t) within each dialysis cassette was determined spectrophotometrically
32 (SHIMADZU, Japan). The free ligand concentration (C_f) was determined
33 spectrophotometrically using an aliquot of the dialysate solution. The amounts of
34 bound compounds were determined by the difference between the total ligand
35 concentration and the free ligand concentration ($C_b=C_t - C_f$). Final analysis of the data
36 was carried out by GraphPad Prism 6.0 software (GraphPad Software, Inc., USA).
37
38
39
40
41
42
43
44
45
46
47
48
49
50
51
52
53
54
55
56
57
58
59
60

1
2
3 **Microscale thermophoresis (MST).** The 5'-end FAM labeled Pu22 and
4 duplex sequences were purchased from Invitrogen (China). The thermophoresis
5 movements of the fluorescent-labeled nucleic acids and compound complexes were
6 detected by monitoring the fluorescence distributions inside the capillary by using the
7 NT.115 MST machine (NanoTemper, Germany). The concentrations of FAM-Pu22
8 and FAM-Duplex were held constant at approximately 0.5 μM , and the compound
9 was diluted at 1:2 from 500 μM 16 times. The samples were loaded into
10 standard-treated MST-grade glass capillaries. The intensities of the LED and laser
11 were set as 40% and 60%, respectively. Data were analyzed using NT Analysis 1.4.23.
12 Software.
13
14
15
16
17
18
19
20
21
22
23
24
25
26

27 **Circular dichroism spectroscopy (CD).** Studies were performed on a
28 Chirascan[®] circular dichroism spectrophotometer (Applied Photophysics, UK). A
29 quartz cuvette with a 4-mm path length was used for the recording of spectra over a
30 wavelength range of 230-330 nm with a 1 nm bandwidth, 1 nm step size and time of
31 0.5 s per point. The DNA samples were set at the concentration of 3 μM . A buffer
32 baseline was collected in the same cuvette and subtracted from the sample spectra.
33 Final analysis of the data was conducted using GraphPad Prism 6.0 (GraphPad
34 Software, Inc).
35
36
37
38
39
40
41
42
43
44
45
46

47 **Molecular docking.** The solution structures of *c-myc* G-quadruplex bound to
48 quindoline molecule (PDB code: 2L7V, authors will release the atomic coordinates
49 and experimental data upon article publication) were used as the target for docking
50 studies. The ligand found in the *c-myc* complex was removed from the structure to
51 leave empty binding sites. After optimizing the ligand and assigning partial atomic
52
53
54
55
56
57
58
59
60

1
2
3 charges, docking calculations were performed with Glide of the Maestro suite in
4
5 extra-precision (XP) mode. The relaxation of all-atom docking structures obtained is
6
7 then implemented under MacroModel from Schrödinger using Steepest Descent
8
9 followed by Truncated Newton Conjugate Gradient until the root mean square (RMS)
10
11 of the energy gradient reaches a value of 0.01 kcal/mol/Å in an OPLS 2005 force field
12
13 and a distance-dependent dielectric.
14
15
16
17

18 **MTT assay.** Hela cervical cancer cells, A549 lung adenocarcinoma cells, Raji
19
20 and CA46 lymphoma cells and primary cultured mouse mesangial cells were seeded
21
22 on 96-well plates (5.0×10^3 /well) and exposed to various concentrations of
23
24 compounds. After 48 h of treatment at 37 °C in a humidified atmosphere of 5% CO₂,
25
26 20 µL of 2.5 mg/mL methyl thiazolyl tetrazolium (MTT) solution was added to each
27
28 well and further incubated for 4 h. The cells in each well were then treated with
29
30 dimethyl sulfoxide (DMSO) (200 µL for each well) and the optical density (OD) was
31
32 recorded at 570 nm. All the experiments were repeated for three times. The
33
34 cytotoxicity was evaluated based on the percentage of cell survival in a
35
36 dose-dependent manner regard to the negative control. The final IC₅₀ values were
37
38 calculated by using the GraphPad Prism 6.0 (GraphPad Software, Inc).
39
40
41
42
43
44

45 **Real-time cellular analysis (RTCA) assay.** A549 cells or primary cultured
46
47 mouse mesangial cells were seeded at 1500 cells per well in E-Plate 16-well plates
48
49 (Roche Applied Science, Indianapolis, IN). The cells were monitored using the
50
51 xCELLigence DP system (Roche Applied Science, Indianapolis, IN) at 15 min
52
53 intervals. After 24 h of RTCA profiling, the assay was paused, and the E-Plate was
54
55 removed from the xCELLigence system. The existing media was carefully removed
56
57
58
59
60

1
2
3 and replaced with the new media with different concentrations of compounds. The
4
5 E-Plate was placed back into the xCELLigence system and cells were monitored for a
6
7 total 100 h. Results were plotted using the RTCA software 1.2 (Roche Applied
8
9 Science, Indianapolis, IN). The data expressed in cell index (CI) units was exported to
10
11 GraphPad Prism 6.0 (GraphPad Software, Inc) for mathematical analysis and
12
13 normalization.
14
15

16
17
18 **Dual-luciferase reporter assay.** For this assay, 200 ng of constructed
19
20 psiCHECK2 luciferase plasmid (Promega, USA) containing *c-myc* promoter, or other
21
22 wild-type and mutant promoters, was transfected into Raji cells using Lipofectamine
23
24 2000 (Invitrogen, USA). After 4 h, compounds were added to the cells at
25
26 concentrations depending on their IC₅₀ values in the MTT assay. The cells were
27
28 incubated at 37 °C with CO₂ for another 24 h, and the transfected cells were first
29
30 washed with ice-cold PBS to reduce the background signals from the medium.
31
32 Luciferase assays were subsequently performed according to the manufacturer's
33
34 instructions using the Dual-Luciferase Assay System (Promega, USA). After a 3-s
35
36 delay, secreted luciferase signals were collected for 10 s using a microplate reader
37
38 (Molecular Devices, Flex Station 3, USA). The quantification was performed using a
39
40 multimode reader (Molecular Devices). The secreted *Renilla* luciferase activity was
41
42 normalized to the Firefly luciferase activity.
43
44
45
46
47
48

49 **RNA extraction, RT-PCR, and Exon-specific amplification.** Raji, Ramos
50
51 or CA46 cells were seeded in 6-well plate (2×10^5 cells/well) and compounds were
52
53 added at indicating concentrations, or with medium as control. After incubation for 6
54
55 h, cells were harvested, and the RNA was extracted according to the manufacturer's
56
57
58
59
60

1
2
3 instructions. Total RNA was used as a template for reverse transcription using the
4 following protocol: each 20 μ L reaction contained 4 μ L 5 \times M-MLV buffer, 2 μ L 2.5
5 mM dNTP, 2 μ L 100 pM oligo dT18 primer, 1 mL M-MLV reverse transcriptase, 0.5
6 μ L 40 U/mL RNase inhibitor, DEPC treated water (DEPC H₂O), and 2 μ g of total
7 RNA. Briefly, RNA and oligo dT18 primer were incubated at 70 °C for 10 min, and
8 then immediately placed on ice. Next, the other components were added, and
9 incubated at 42 °C for 1 h, and then at 70 °C for 15 min. The cDNA was applied
10 directly for further PCR or exon-specific amplification. The PCR reaction was
11 performed in an apparatus (effendorf), and the PCR products were analyzed with
12 electrophoresis on 1.5% agarose gel at 120 V for 40 min. The real-time PCR was
13 performed on a real-time PCR apparatus (Roche LightCycler 480) by using SYBR
14 Premix Ex Taq (Takara), according to the manufacturer's protocol. The total of
15 volume of 20 μ L quantitative reaction mixtures containing 10 μ L of SYBR Green Mix
16 (TOYOBO, Japan), 0.5 μ M of each primer, and 1 μ L of cDNA. The exon 1 and exon
17 2 mRNAs were normalized to β -actin mRNA level of each sample. Results of
18 real-time PCR were analyzed using $2^{-\Delta\text{CT}}$ method.
19
20
21
22
23
24
25
26
27
28
29
30
31
32
33
34
35
36
37
38
39
40

41 **Western blot.** Raji cells harvested from each well of the culture plates were
42 lysed in 100 μ L of extraction buffer. The suspension was centrifuged at 12,000 rpm at
43 4 °C for 10 min, and then quantitated by using BCA. Total protein lysates (20 μ g)
44 were electrophoresed on 8% SDS-PAGE and transferred to a PVDF membrane at 100
45 V for 1.5 h. The membrane was blocked for 1 h with 5% solution Bovine Serum
46 Albumin in TBS, 0.05% Tween at room temperature. Western blotting was performed
47 using anti- C-MYC (Cell Signaling Technology: 5605S), anti-GAPDH (Cell
48 Signaling Technology: 14C10) primary antibody and
49
50
51
52
53
54
55
56
57
58
59
60

1
2
3 horseradish-peroxidase-conjugated anti-rabbit secondary antibody. The protein bands
4
5 were visualized using chemiluminescence substrate.
6
7

8
9
10 **Cell cycle arrest assay.** The Raji cells were incubated in 10%
11 FBS-supplemented 1640 culture medium with compound **5a**, **5h** and **5l** at 1 μ M for 6
12 h at 37 °C and 5% CO₂. After treatment, cells were collected and fixed with ice-cold
13 70% ethanol at -20 °C overnight. Fixed cells were re-suspended in 0.5 mL of PBS
14 containing 50 mg/mL propidium iodide. The cell cycle distribution was analyzed by
15 using EPICS XL flow cytometer and calculated by using EXPO 32 software.
16
17
18
19
20
21
22
23

24
25 **Xenograft animal model and drug treatments.** BALB/c female and male
26 nude mice were obtained from the laboratory animal centre of Sun Yat-sen University.
27 A549 cells were harvested, pelleted by centrifugation at 800 g for 5 min, and
28 re-suspended in sterile serum-free medium without EDTA. The cells (1×10^7 in 100 μ L)
29 were then subcutaneously implanted into the underarm regions of two mice. After the
30 tumours grew to almost 1000 mm³, the tumour tissues were removed and divided.
31 Then, the divided tissues were implanted into the underarm regions of 15 mice. These
32 mice were separated into three groups: control, compound **7**-treated, compound
33 **5l**-treated, and positive control (doxorubicin-treated). Compound **5l** and **7**,
34 doxorubicin, and saline were administered by i.p. injection to athymic nude mice with
35 human tumour xenografts established using A549 lung cancer cells. Mice were
36 injected i.p. once a day for 12 days. Control group was injected with 150 μ L of saline.
37 The positive control group received doxorubicin by i.p. injection at a dose of 1 mg/Kg.
38 Compound **5l** and **7** were similarly administered to mice at a dose of 6.26 mg/Kg, and
39 7.5 mg/Kg, respectively. After treating the animals for 12 days, the tumour tissues
40
41
42
43
44
45
46
47
48
49
50
51
52
53
54
55
56
57
58
59
60

1
2
3 were collected, and IHC assays were conducted using an anti-cMyc antibody
4
5 according to a general procedure.
6
7
8
9

10 ■ ACKNOWLEDGMENTS

11
12 This work was supported by the National Natural Science Foundation of China
13 (21372263 and 81673286 for T.-M. Ou; 81330077 for Z.-S. Huang), the Foundation
14
15 for Distinguished Young Talents in Higher Education of Guangdong (Yq2013002 for
16
17 T.-M. Ou), and Guangdong Provincial Key Laboratory of Construction Foundation
18
19 (Grant 2011A060901014) for financial support of this study.
20
21
22
23
24
25
26
27

28 ■ AUTHOR INFORMATION

29 30 Corresponding Author

31
32 * For Tian-Miao Ou: phone, 8620-39943053; e-mail, outianm@mail.sysu.edu.cn.
33
34
35

36 Author Contributions

37
38 † These authors contributed equally.
39
40
41
42
43

44 ■ ABBREVIATIONS

45
46 CD, circular dichroism; FRET, fluorescence resonance energy transfer; MST,
47
48 microscale thermophoresis; NHE III₁, nuclease-hypersensitive element; RTCA,
49
50 real-time cellular analysis; SAR, structure-activity relationship.
51
52
53
54
55

56 ■ ASSOCIATED CONTENT

57
58
59
60

Supporting Information

Additional experimental results, ^1H and ^{13}C NMR spectra, HRMS, HPLC assay data for final compounds, and the Molecular Formula Strings are available free of charge via the Internet at <http://pubs.acs.org>. PDB ID Codes was 2L7V, and authors will release the atomic coordinates and experimental data upon article publication.

■ REFERENCES

1. Bacolla, A.; Wells, R. D., Non-B DNA conformations as determinants of mutagenesis and human disease. *Mol. Carcinogen.* **2009**, *48* (4), 273-285.
2. Burge, S.; Parkinson, G. N.; Hazel, P.; Todd, A. K.; Neidle, S., Quadruplex DNA: sequence, topology and structure. *Nucleic Acid Res.* **2006**, *34* (19), 5402-5415.
3. Chambers, V. S.; Giovanni, M.; Boutell, J. M.; Marco, D. A.; Smith, G. P.; Shankar, B., High-throughput sequencing of DNA G-quadruplex structures in the human genome. *Nat. Biotechnol.* **2015**, *33* (8), 877-881.
4. Balasubramanian, S.; Neidle, S., G-quadruplex nucleic acids as therapeutic targets. *Curr. Opin. Chem. Biol.* **2009**, *13* (3), 345-353.
5. Neidle, S., Quadruplex nucleic acids as novel therapeutic \geq ?,targets. *J. Med. Chem.* **2016**, *59* (13), 5987-6011.
6. Dang, C. V.; Resar, L. M.; Emison, E.; Kim, S.; Li, Q.; Prescott, J. E.; Wonsey, D.; Zeller, K., Function of the c-Myc oncogenic transcription factor. *Exp. Cell Res.* **1999**, *253* (1), 63-77.
7. Simonsson, T.; Kubista, M.; Pecinka, P., DNA tetraplex formation in the control region of c-myc.

1
2
3
4
5
6
7
8
9
10
11
12
13
14
15
16
17
18
19
20
21
22
23
24
25
26
27
28
29
30
31
32
33
34
35
36
37
38
39
40
41
42
43
44
45
46
47
48
49
50
51
52
53
54
55
56
57
58
59
60

Nucleic Acid Res. **1998**, *26* (5), 1167-1172.

8. Tomonaga, T.; Levens, D., Activating transcription from single stranded DNA. *P. Natl. Acad. Sci. U.S.A.* **1996**, *93* (12), 5830-5835.

9. Siddiqui-Jain, A.; Grand, C. L.; Bearss, D. J.; Hurley, L. H., Direct evidence for a G-quadruplex in a promoter region and its targeting with a small molecule to repress c-MYC transcription. *P. Natl. Acad. Sci. U.S.A.* **2002**, *99* (18), 11593-11598.

10. Sun, D.; Hurley, L. H., The importance of negative superhelicity in inducing the formation of G-quadruplex and i-motif structures in the c-Myc promoter: implications for drug targeting and control of gene expression. *J. Med. Chem.* **2009**, *52* (9), 2863-2874.

11. Seenisamy, J.; Bashyam, S.; Gokhale, V.; Vankayalapati, H.; Sun, D.; Siddiqui-Jain, A.; Streiner, N.; Shin-Ya, K.; White, E.; Wilson, W. D., Design and synthesis of an expanded porphyrin that has selectivity for the c-MYC G-quadruplex structure. *J. Am. Chem. Soc.* **2005**, *127* (9), 2944-2959.

12. Ou, T.-M.; Lin, J.; Lu, Y.-J.; Hou, J.-Q.; Tan, J.-H.; Chen, S.-H.; Li, Z.; Li, Y.-P.; Li, D.; Gu, L.-Q.; Huang, Z.-S., Inhibition of cell proliferation by quindoline derivative (SYUIQ-05) through its preferential interaction with c-myc promoter G-quadruplex. *J. Med. Chem.* **2011**, *54* (16), 5671-5679.

13. Ma, Y.; Ou, T.-M.; Tan, J.-H.; Hou, J.-Q.; Huang, S.-L.; Gu, L.-Q.; Huang, Z.-S., Quinolino-benzo-[5, 6]-dihydroisoquinolium compounds derived from berberine: a new class of highly selective ligands for G-quadruplex DNA in c-myc oncogene. *Eur. J. Med. Chem.* **2011**, *46* (5), 1906-1913.

14. Amato, J.; Morigi, R.; Pagano, B.; Pagano, A.; Ohnmacht, S. A.; De Magis, A.; Tiang, Y.-P.; Capranico, G.; Locatelli, A.; Graziadio, A.; Leoni, A.; Rambaldi, M.; Novellino, E.; Neidle, S.; Randazzo, A., Toward the development of specific G-quadruplex binders: synthesis, biophysical and

- 1
2
3
4 biological studies of new hydrazone derivatives. *J. Med. Chem.* **2016**, *59* (12), 5706-5720.
- 5
6 15. Guyen, B.; Schultes, C. M.; Hazel, P.; Mann, J.; Neidle, S., Synthesis and evaluation of analogues
7
8 of 10H-indolo[3,2-b]quinoline as G-quadruplex stabilising ligands and potential inhibitors of the
9
10 enzyme telomerase. *Org. Biomol. Chem.* **2004**, *2* (7), 981-988.
- 11
12
13 16. Long, Y.; Li, Z.; Tan, J. H.; Ou, T. M.; Li, D.; Gu, L. Q.; Huang, Z. S., Benzofuroquinoline
14
15 derivatives had remarkable improvement of their selectivity for telomeric G-quadruplex DNA over
16
17 duplex DNA upon introduction of peptidyl group. *Bioconjugate Chem.* **2012**, *23* (9), 1821-31.
- 18
19
20 17. Lu, Y. J.; Ou, T. M.; Tan, J. H.; Hou, J. Q.; Shao, W. Y.; Peng, D.; Sun, N.; Wang, X. D.; Wu, W.
21
22 B.; Bu, X. Z.; Huang, Z. S.; Ma, D. L.; Wong, K. Y.; Gu, L. Q., 5-N-methylated quindoline derivatives
23
24 as telomeric g-quadruplex stabilizing ligands: effects of 5-N positive charge on quadruplex binding
25
26 affinity and cell proliferation. *J. Med. Chem.* **2008**, *51* (20), 6381-6392.
- 27
28
29 18. Ou, T. M.; Lu, Y. J.; Zhang, C.; Huang, Z. S.; Wang, X. D.; Tan, J. H.; Chen, Y.; Ma, D. L.; Wong,
30
31 K. Y.; Tang, J. C.; Chan, A. S.; Gu, L. Q., Stabilization of G-quadruplex DNA and down-regulation of
32
33 oncogene c-myc by quindoline derivatives. *J. Med. Chem.* **2007**, *50* (7), 1465-1474.
- 34
35
36 19. Wang, X. D.; Ou, T. M.; Lu, Y. J.; Li, Z.; Xu, Z.; Xi, C.; Tan, J. H.; Huang, S. L.; An, L. K.; Li, D.;
37
38 Gu, L. Q.; Huang, Z. S., Turning off transcription of the bcl-2 gene by stabilizing the bcl-2 promoter
39
40 quadruplex with quindoline derivatives. *J. Med. Chem.* **2010**, *53* (11), 4390-4398.
- 41
42
43 20. Wu, Y.; Zan, L. P.; Wang, X. D.; Lu, Y. J.; Ou, T. M.; Lin, J.; Huang, Z. S.; Gu, L. Q.,
44
45 Stabilization of VEGF G-quadruplex and inhibition of angiogenesis by quindoline derivatives.
46
47 *BBA-Gen Subjects* **2014**, *1840* (9), 2970-2977.
- 48
49
50 21. Zhou, J. L.; Lu, Y. J.; Ou, T. M.; Zhou, J. M.; Huang, Z. S.; Zhu, X. F.; Du, C. J.; Bu, X. Z.; Ma,
51
52 L.; Gu, L. Q.; Li, Y. M.; Chan, A. S., Synthesis and evaluation of quindoline derivatives as
53
54
55
56
57
58
59
60

- 1
2
3
4 G-quadruplex inducing and stabilizing ligands and potential inhibitors of telomerase. *J. Med. Chem.*
5
6 **2005**, *48* (23), 7315-7321.
7
8
9 22. Dai, J.; Carver, M.; Hurley, L. H.; Yang, D., Solution structure of a 2:1 quindoline-c-MYC
10
11 G-quadruplex: insights into G-quadruplex-interactive small molecule drug design. *J. Am. Chem. Soc.*
12
13 **2011**, *133* (44), 17673-17680.
14
15
16 23. Lauria, A.; Delisi, R.; Mingoia, F.; Terenzi, A.; Martorana, A.; Barone, G.; Almerico, A. M.,
17
18 1,2,3-Triazole in heterocyclic compounds, endowed with biological activity, through 1,3-dipolar
19
20 cycloadditions. *Eur. J. Org. Chem.* **2014**, *2014* (16), 3289-3306.
21
22
23 24. Agalave, S. G.; Maujan, S. R.; Pore, V. S., Click chemistry: 1,2,3-triazoles as pharmacophores.
24
25
26 *Chem.-Asian J.* **2011**, *6* (10), 2696-2718.
27
28
29 25. Moorhouse, A. D.; Santos, A. M.; Gunaratnam, M.; Moore, M.; Neidle, S.; Moses, J. E.,
30
31 Stabilization of G-quadruplex DNA by highly selective ligands via click chemistry. *J. Am. Chem. Soc.*
32
33 **2006**, *128* (50), 15972-15973.
34
35
36 26. Ritson, D. J.; Moses, J. E., A fragment based click chemistry approach towards hybrid
37
38 G-quadruplex ligands: design, synthesis and biophysical evaluation. *Tetrahedron* **2012**, *68* (1),
39
40 197-203.
41
42
43 27. Sparapani, S.; Haider, S. M.; Doria, F.; Gunaratnam, M.; Neidle, S., Rational design of
44
45 acridine-based ligands with selectivity for human telomeric quadruplexes. *J. Am. Chem. Soc.* **2010**, *132*
46
47 (35), 12263-12272.
48
49
50
51 28. Drewe, W. C.; Neidle, S., Click chemistry assembly of G-quadruplex ligands incorporating a
52
53 diarylurea scaffold and triazole linkers. *Chem. Commun.* **2008**, *42*, 5295-5297.
54
55
56
57 29. Di Antonio, M.; Biffi, G.; Mariani, A.; Raiber, E. A.; Rodriguez, R.; Balasubramanian, S.,
58
59
60

1
2
3
4 Selective RNA versus DNA G-quadruplex targeting by in situ click chemistry. *Angew. Chem. Int. Ed.*

5
6 **2012**, *51* (44), 11073-11078.

7
8
9 30. Rezler, E. M.; Seenisamy, J.; Bashyam, S.; Kim, M. Y.; White, E.; Wilson, W. D.; Hurley, L. H.,

10
11 Telomestatin and diseleno saphyrin bind selectively to two different forms of the human telomeric

12
13 G-quadruplex structure. *J. Am. Chem. Soc.* **2005**, *127* (26), 9439-9447.

14
15
16 31. Jerabek-Willemsen, M.; Wienken, C. J.; Braun, D.; Baaske, P.; Duhr, S., Molecular interaction
17
18 studies using microscale thermophoresis. *Assay Drug Dev. Technol.* **2011**, *9* (4), 342-353.

19
20
21 32. Brooks, T. A.; Hurley, L. H., Targeting MYC expression through G-quadruplexes. *Genes Cancer*

22
23 **2010**, *1* (6), 641-649.

24
25
26 33. Robert V. Brown, F. L. D., Vijay Gokhale, Laurence H. Hurley, Tracy A. Brooks, Demonstration

27
28 that drug-targeted down-regulation of MYC in non-hodgkins lymphoma is directly mediated through

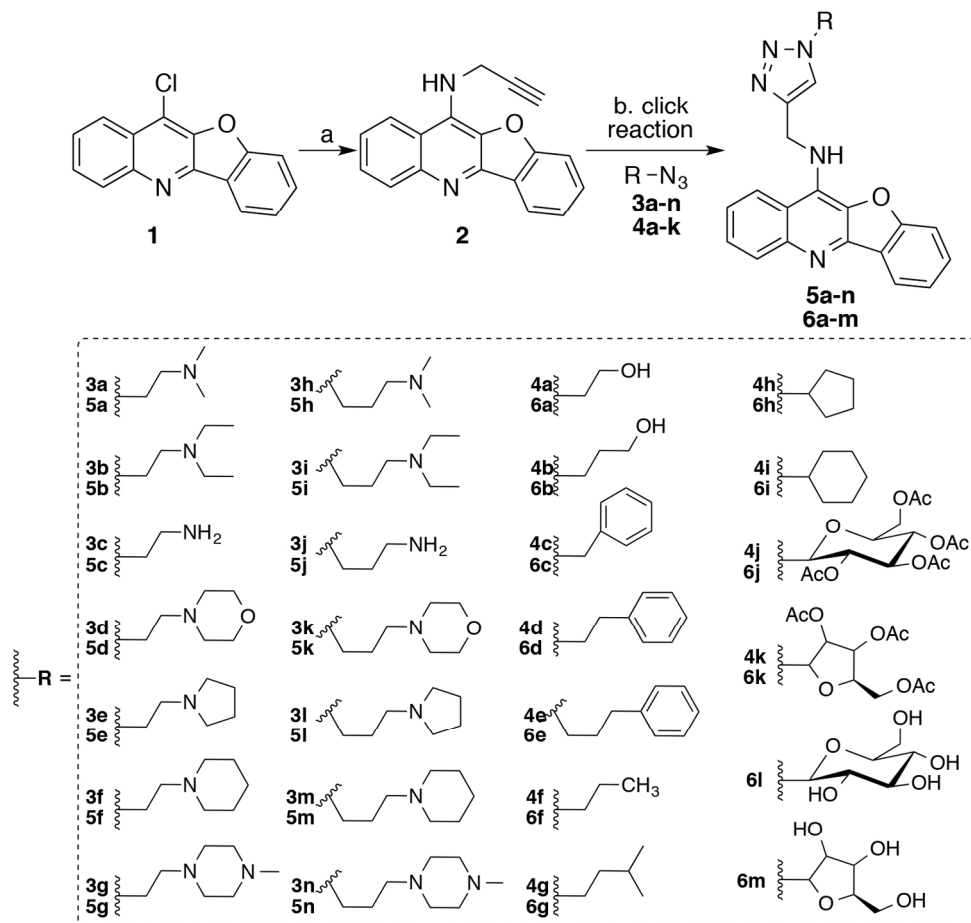
29
30 the promoter G-quadruplex. *J. Biol. Chem.* **2011**, *286* (47), 41018-41027.

31
32
33 34. Mergny, J. L.; Maurizot, J. C., Fluorescence resonance energy transfer as a probe for G-quartet

34
35 formation by a telomeric repeat. *ChemBioChem* **2001**, *2* (2), 124-132.

36
37
38 35. Ragazon, P.; Chaires, J. B., Use of competition dialysis in the discovery of G-quadruplex

39
40 selective ligands. *Methods* **2007**, *43* (4), 313-23.
41
42
43
44
45
46
47
48
49
50
51
52
53
54
55
56
57
58
59
60



38 Scheme 1. Synthesis of 11-triazole benzofuro[3,2-b]-quinoline derivatives **5a-n**, and **6a-m**. Reagents and
39 conditions: (a) p-TsOH, 2-Propargylamine, 120 oC, 6 hours; (b) Azides **3a-n** and **4a-k**, CuSO₄·5H₂O, sodium
40 ascorbate, THF/H₂O, 35 oC, 6-12 hours.

41 145x135mm (300 x 300 DPI)

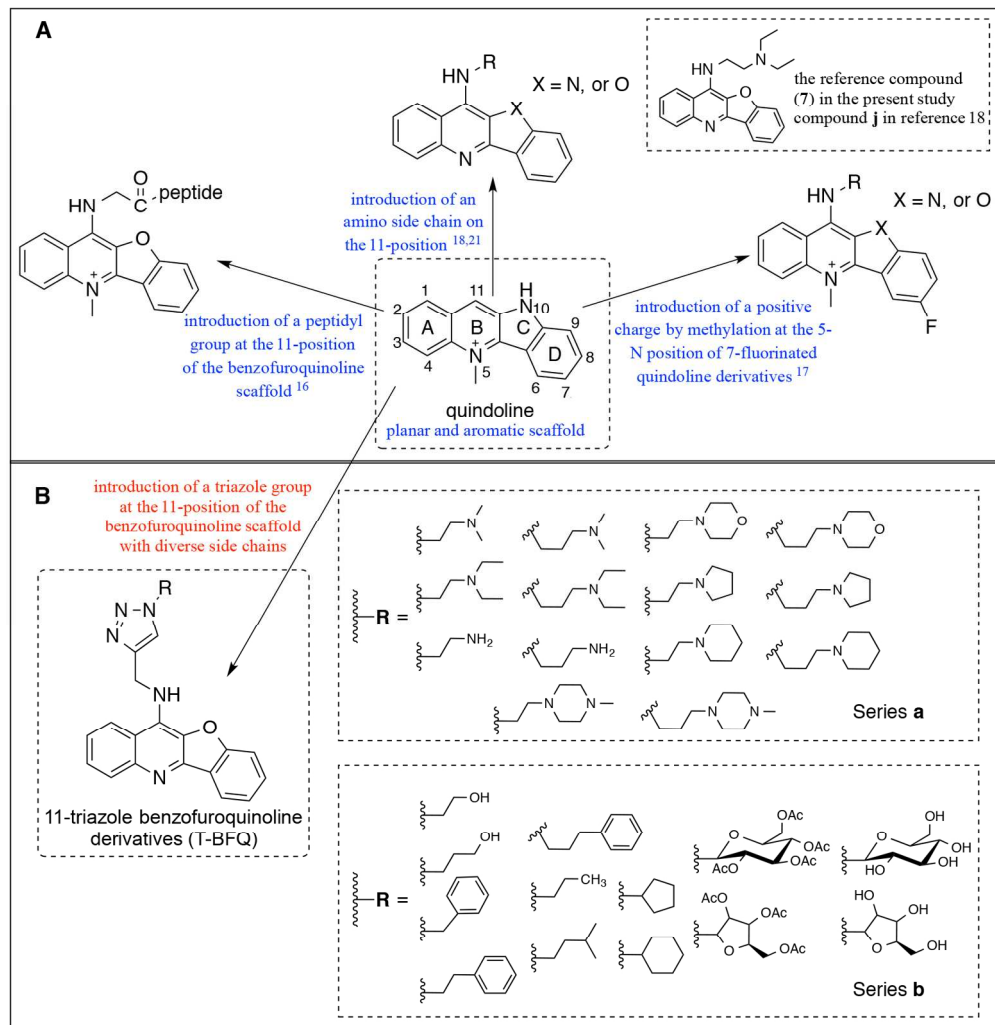


Figure 1. Modification strategies of the quindoline scaffold in previous studies (A) and the present study (B).

156x162mm (300 x 300 DPI)

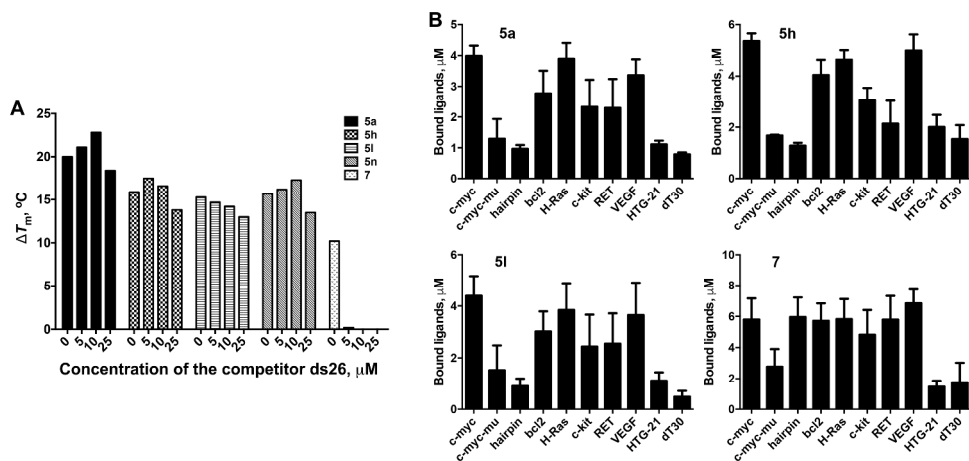


Figure 2. A. Competitive FRET results for T-BFQ derivatives 5a, 5h, 5l, and 5n without and with 5-fold (2 μM), 10-fold (4 μM) or 25-fold (10 μM) excess of duplex DNA competitor (ds26). The concentration of FPU22T was 0.4 μM . B. Competition dialysis results of T-BFQ derivatives 5a, 5h, and 5l, and the reference compound 7 binding to the c-myc G-quadruplex or other DNA oligomers. A 10 mM Tris-HCl buffer (pH 7.4) containing 100 mM NaCl was used in the experiments.

350x164mm (300 x 300 DPI)

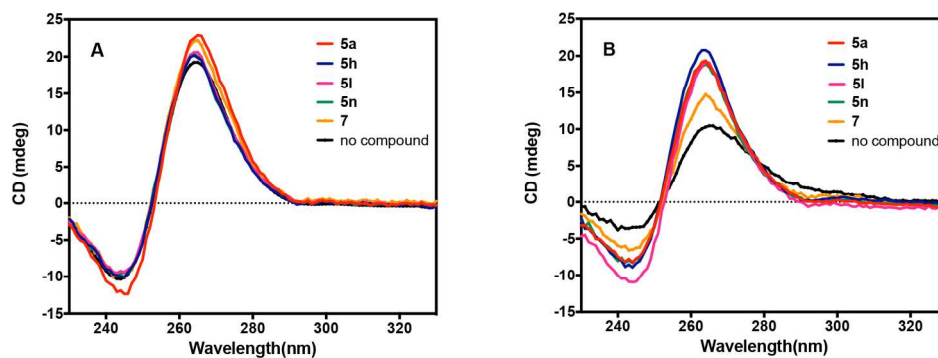


Figure 3. CD spectra of Pu22 (5 μ M) in 10 mM Tris-HCl buffer (pH 7.4) in the presence of 100 mM KCl (A), and in the absence of KCl (B). CD spectra of Pu22 (black line), and Pu22 in the presence of 5 μ M of 5a, 5h, 5l, 5n, and 7, respectively.

165x63mm (300 x 300 DPI)

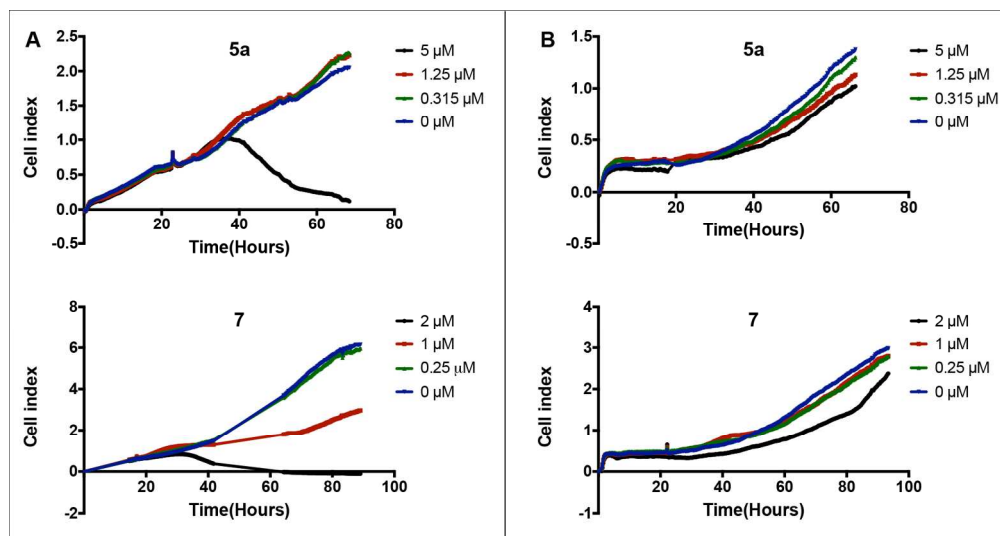


Figure 4. The effect of compound 5a and 7 on the proliferation of A549 cells (A) and primary cultured mouse mesangial cells (B) measuring by using RTCA assay. A549 lung adenocarcinoma cells and primary cultured mouse mesangial cells were seeded (2000 cells each well) on E-Plate 16 PET culturing about 20 h before compound treatment. Cells were treated with various concentrations of 5a, 7, or DMSO control.

165x87mm (300 x 300 DPI)

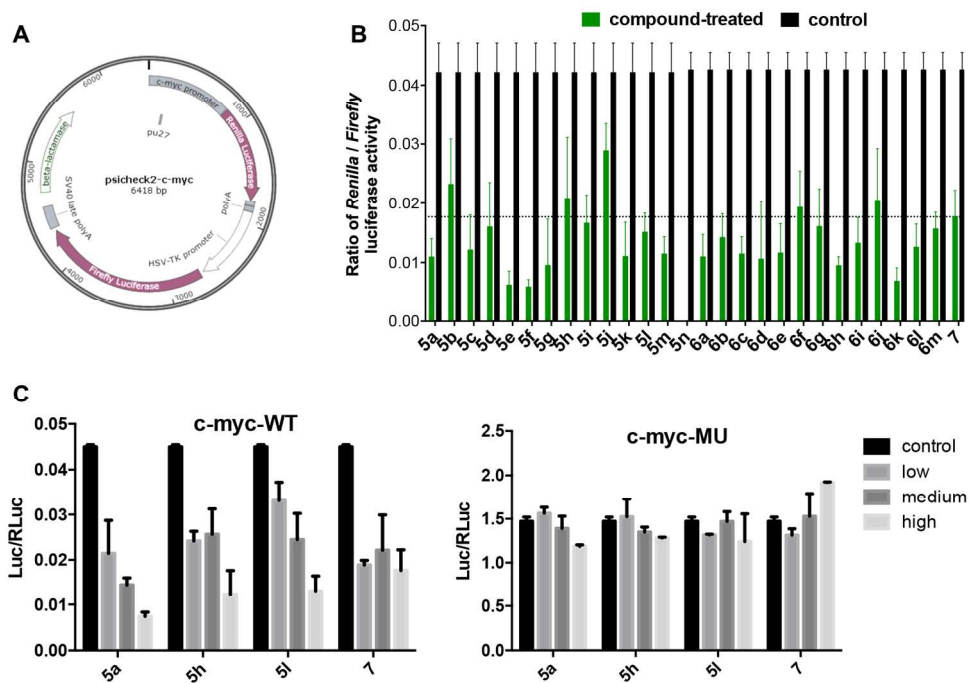


Figure 5. The effects of T-BFQ derivatives on c-myc promoter's activity via dual luciferase reporter assays. (A) Schematic diagram of the plasmids used in dual luciferase reporter assays. The psiCHECK2 plasmid carrying the c-myc promoter in front of the Renilla luciferase, and the Firefly luciferase in the same plasmid, was transfected into cells. (B) Column graph showing the relative expression level of the Renilla luciferase (activity of Renilla luciferase/activity of Firefly luciferase) after the addition of T-BFQ derivatives. All the experiments were repeated for three times. (C) Column graph showing the relative expression level of the Renilla luciferase (activity of Renilla luciferase/activity of Firefly luciferase) in plasmids containing wild-type or mutant constructs after the addition of T-BFQ derivatives. Cells were treated with 1/8 IC₅₀ (low), 1/2 IC₅₀ (medium), and IC₅₀ (high) of compounds. All the experiments were repeated for three times.

150x103mm (300 x 300 DPI)

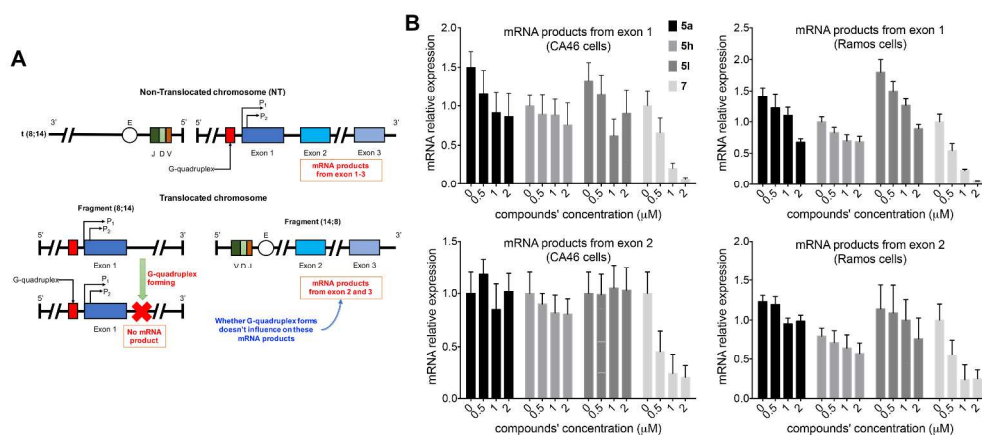


Figure 6. Effects of T-BFQ derivatives on c-myc's translocation. (A) Exon-specific expression in Raji cells based on translocation events. (B) Real-time RT-PCR results of Exon-specific expression in CA46 and Ramos cells upon addition of compound 5a, 5h, 5l, and 7 with concentrations from 0 to 2 μM . mRNA relative expression was calculated with ct values and columned in graph. All the experiments were repeated for three times.

323x139mm (300 x 300 DPI)

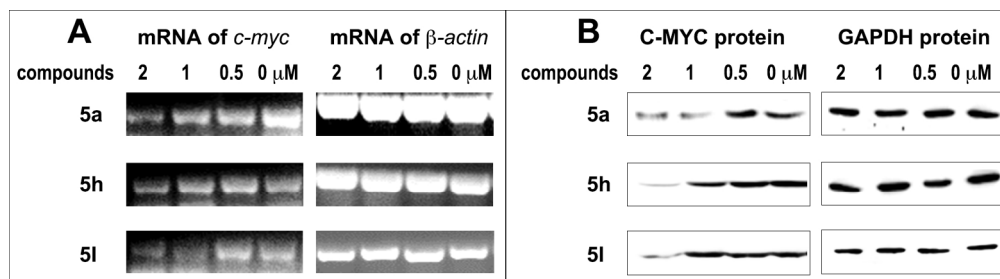


Figure 7. The Effects of 5a, 5h and 5l on *c-myc* transcription and expression after 96 h treatment in Raji cells. (A) The transcription level of *c-myc* gene in the presence of 5a, 5h and 5l in Raji cells by using RT-PCR. β -actin was used as an internal control. All the experiments were repeated for three times. (C) Expression level of C-MYC protein under the treatment of increased concentrations of 5a, 5h and 5l in Raji cells by using Western blot. β -Actin was used as an internal control. All the experiments were repeated for three times.

168x46mm (300 x 300 DPI)

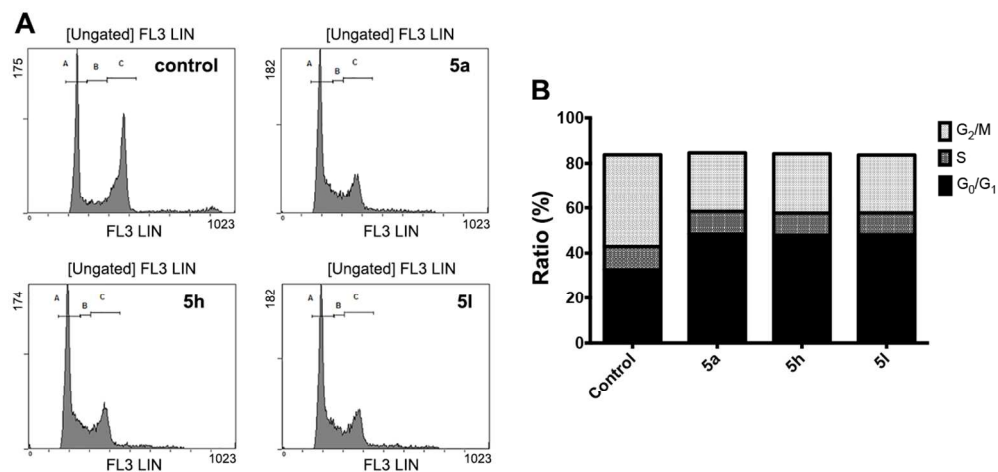


Figure 8. The induction of G₀/G₁ phase arrest in Raji cells by compounds 5a, 5h and 5l. (A) Cell cycle analysis after propidium iodide (PI) staining after 6-h treatment with 1 μ M 5a, 5h, and 5l, or 0.1% DMSO in Raji cells. (B) The percentage of cells in different phases of the cell cycle, analyzed by EXPO32 ADC software. All the experiments were repeated for three times.

112x54mm (300 x 300 DPI)

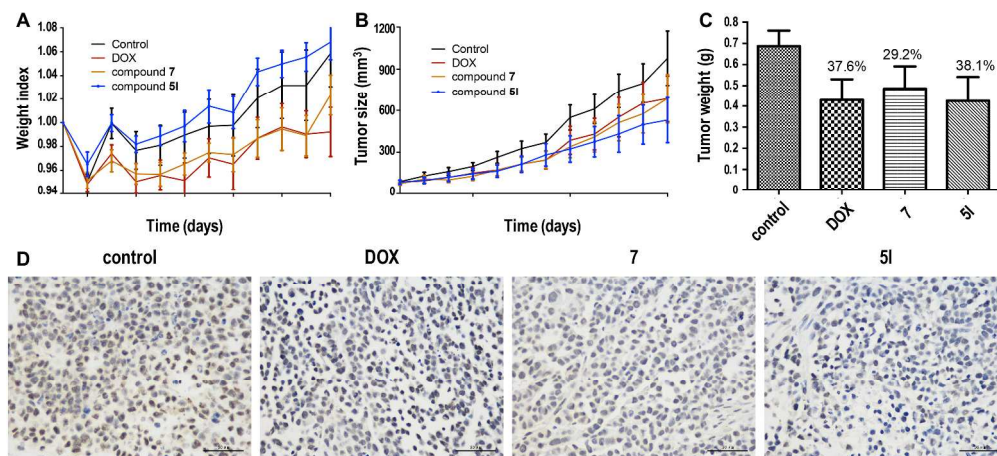


Figure 9. Compound 5I and 7, doxorubicin, and saline were administered by i.p. injection to athymic nude mice with human tumor xenografts established using A549 lung cancer cells. The mice were injected i.p. once a day for 12 days. The control group was injected with 150 μ L of saline. The positive control group (DOX) received doxorubicin by i.p. injection at a dose of 1 mg/Kg, once two days for 12 days. Compound 5I and 7 were similarly administered to mice, once a day, at a dose of 6.25 mg/Kg, and 7.5 mg/Kg, respectively. The body weight (A) and tumor volume (B) were recorded every two days, and the tumor weight was evaluated when the treatment ended (C). The inhibition rate was calculated using (tumor weight in drug-treatment group) / (tumor weight in control group) and indicated on the column. (D) The expression of c-Myc protein was identified by IHC, and pictures were taken at 400 \times magnification. Images of three independent samples in each group were selected and presented for to give an overall illustration of the results.

326x156mm (300 x 300 DPI)

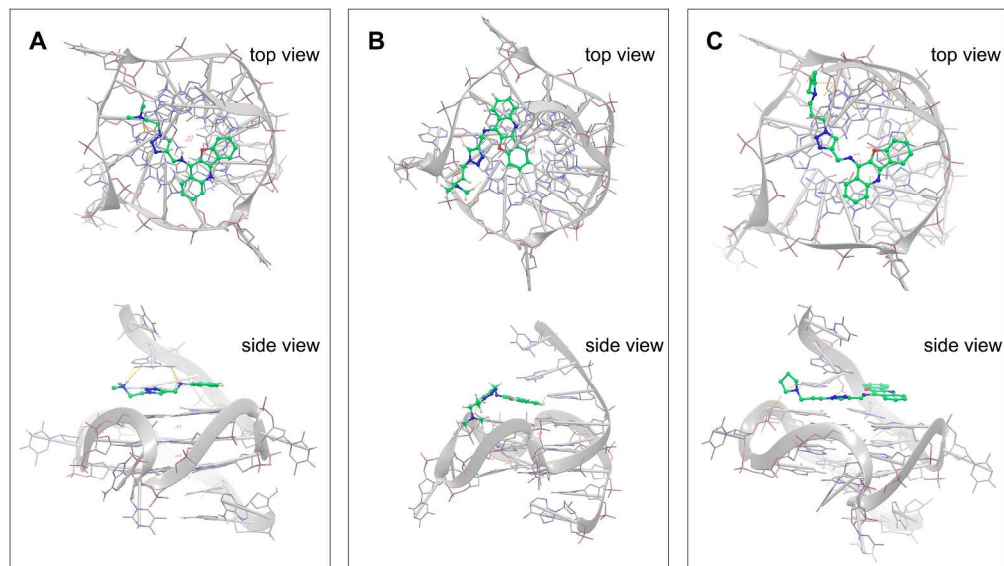


Figure 10. Docking results of derivatives 5a (A), 5h (B), and 5l (C) onto the c-myc G-quadruplex (top views onto the 5' of the c-myc G-quadruplex and side views, PDB code: 2L7V, authors will release the atomic coordinates and experimental data upon article publication).

259x146mm (300 x 300 DPI)

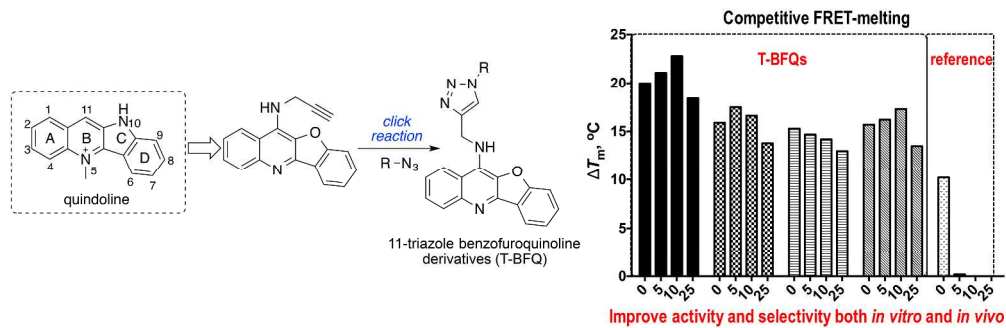


Table of contents graphic

350x115mm (300 x 300 DPI)